Engineering Structures 323 (2025) 119288

Contents lists available at ScienceDirect

Engineering Structures

journal homepage: www.elsevier.com/locate/engstruct

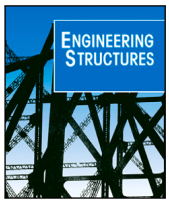

An accurate and ready-to-use approach for the estimation of impedance functions of regular pile groups for offshore wind turbine foundations. Vertical and rocking components

Eduardo Rodríguez-Galván, Guillermo M. Álamo *, Juan J. Aznárez, Orlando Maeso

Instituto Universitario de Sistemas Inteligentes y Aplicaciones Numéricas en Ingeniería (SIANI), Universidad de Las Palmas de Gran Canaria, 35017, Las Palmas de Gran Canaria, Spain

ARTICLE INFO

Keywords:
Pile groups
Group impedances
Interaction factor
Pile-to-pile interaction
Dynamic analysis
Offshore Wind Turbines

ABSTRACT

The interaction factor superposition method in the determination of the vertical and rocking impedances of pile groups for jacket-supported Offshore Wind Turbines is studied. The vertical and rocking group dynamic impedances obtained by this method are compared with those computed by a previously developed continuum model. The influence of the main parameters that define the problem is also studied. In order to propose an alternative calculation solution, some expressions dependent of these parameters are fitted from an extensive selection of jacket pile group configurations. These expressions allow to estimate the vertical flexibility of the source pile and the interaction factor between a pair of piles. Subsequently, applying elastic superposition, the group impedance functions are determined. Results show that the interaction factor superposition method correctly reproduces the vertical and rocking group dynamic impedances. Therefore, for these regular pile groups with large spacing ratios, the assumption of only considering the direct interaction between pile pairs leads to accurate results. Results obtained with the proposed fitted expressions generally conduct to a good estimation, properly reproducing the variation produced by the influence of the different parameters. Thus, this superposition method and the proposed expressions can be employed to quickly and simply reproduce the vertical soil–structure interaction of this type of structures.

1. Introduction

Pile groups are commonly used in a large variety of structural foundations, such as buildings, bridges and offshore platforms. Within this last group, piles were originally used in oil extraction platforms, but, in recent years, with the search of a sustainable and low-carbon future, they are also employed as Offshore Wind Turbine (OWT) foundations. According to the recent 2023 Global Offshore Wind Report [1], 2021 and 2022 have been the highest years in offshore wind history installation, with 21.1 GW and 8.8 GW of new power installed projects in both years, respectively, representing the 23% and 11% of the total new installations in the last 16 years. The predictions show that this growth will continue and will also be overcome throughout the next ten years. Among all existing offshore wind energy installed projects, monopiles are the most common substructure typology (60.2%) followed by jackets (10.4%) [2]. Although monopiles are expected to keep heading the OWT substructures, it is predicted that jacket substructures will grow to represent 15% of the future market. This increase is assumed by the need of installing OWTs in deeper waters and further from the coast. These jacket substructures are founded on suction caissons or on slender piles. Both suction caissons and piles are located at vertices of a regular polygon, depending on the number of jacket legs. The choice between these two solutions depends on multiple factors such as soil conditions and project-specific requirements. Although suction caissons are faster, cheaper and quieter than piles in terms of installation and removal, pile foundations are more suitable in terms of soil conditions versatility, high load-bearing capacity and settlement control, due to their larger length and vertical and rotational stiffnesses [3].

In this sense, the study of the dynamic response of pile groups is a key problem in the structural design of these devices and the development of this technology. Thus, with other applications, it has already been a widely studied problem over the years. This is a complex problem that involves pile–soil and pile–pile phenomena. The dynamic response of pile groups can be addressed by directly modelling the complete system or by superimposing simple interaction problems. On

* Corresponding author.
E-mail addresses: eduardo.rodriguezgalvan@ulpgc.es (E. Rodríguez-Galván), guillermo.alamo@ulpgc.es (G.M. Álamo), juanjose.aznarez@ulpgc.es (J.J. Aznárez), orlando.maeso@ulpgc.es (O. Maeso).

https://doi.org/10.1016/j.engstruct.2024.119288
Received 3 August 2024; Received in revised form 17 October 2024; Accepted 5 November 2024
Available online 18 November 2024

the one hand, direct models can be carried out with several modelling approaches, such as, the finite element method (FEM), boundary element method (BEM), coupling of these two, or other procedures [4–9]. These direct models exhaustively reproduce pile–pile and pile–soil interactions, but they require a high computational cost. On the other hand, the superposition method is based on estimating the pile group response by superimposing interaction factors [10–15]. The simple nature of this superposition procedure makes it an interesting approach to be used in the design stages and for carrying out parametric studies.

The elastic superposition method (also known as the interaction factor superposition method) was firstly introduced by Poulos [10]. In this work he demonstrated that the static settlement of pile groups can be calculated from simple pile pair configurations, superimposing the source and receiver pile displacements. He also introduced the interaction factor concept as the relation between the receiver (unloaded) and source (loaded) pile displacements. Thereafter, Kaynia [4] studied the dynamic response of pile groups by introducing soil flexibility matrices and pile dynamic stiffness and compared his method with the superposition one, concluding that the Poulos's elastic superposition methodology gives reasonable results either statically and dynamically. Subsequently, Dobry and Gazetas [11] extended Poulos's superposition method to the dynamic analysis of pile groups. This work proposed some frequency dependent expressions to compute the vertical and horizontal displacement of one pile under its own load, as well as the interaction factor. With these expressions pile group dynamic impedances are obtained applying elastic principle of superposition effects. Interaction factors are also employed to simulate pile–soil–pile effects by Winkler models [13,14,16,17], in which Poulos's superposition procedure is then applied. These Winkler approaches can reproduce the interplay between the receiver pile and the soil subjected to the displacement field. Recent works, such as Zheng et al. [18], analysed the scattering and wave diffraction, proposing interaction factors that account these effects.

A large part of the performed works in this area [4,11,15,16,19,20] compared the superposition method with rigorous direct models. Nevertheless, all of them were focused on the analysis of standard pile configurations (square and rectangular arrangements), and not on pile configurations for jacket-supported OWTs, which are characterised by being formed by hollow cylindrical steel piles arranged in N-sided polygonal groups. For this reason, the main scope of this work is to study the interaction factor superposition method in the vertical dynamic response of pile groups for jacket-supported OWTs, considering a wide range of pile group configurations. Three different polygonal pile arrangements are studied, composed of 3, 4 and 5 hollow cylindrical piles embedded in an homogeneous halfspace. The influence of the main variables that intervene in the problem (frequency and pile and soil parameters) is studied. These parameters are considered in order to fit and propose some expressions that allow directly estimating the vertical flexibility of the source pile and the interaction factor of a pair of piles. Then, the dynamic vertical group response is computed applying elastic superposition. In order to carry out the superposition method and fitted expressions, the vertical flexibilities and interaction factors are obtained through a previously developed continuum model [8], which will also be used to verify the final result obtained from the proposed procedure. The proposed expressions allow to reproduce the vertical flexibility of the source pile and the interaction factor of a pair of piles, capturing the influence of the main pile and soil parameters that participate in the problem. These expressions together with the interaction factor superposition method could be useful to compute the vertical and rocking impedances for a wide range of pile groups for jacket-supported OWTs with different pile and soil characteristics. Thus, the overall methodology proposed in this work allows to obtain the vertical and rocking impedance functions in a fast and straightforward way, without the requirement to execute a complex model, with a good level of precision and accounting the influence of all relevant properties of the system. These impedances can be later used in substructuring models or in the design stages of these jacket-supported OWTs, in order to reproduce the soil–structure interaction (SSI). The relevance of considering this interaction has been highlighted in many works [21–25], in which it is emphasised that SSI inclusion plays an important role in the dynamic characteristics of jacket-supported OWTs, mainly in the determination of their natural frequencies, a critical factor in the design of this type of structures.

The present paper is organised in five sections. After the introduction presented in this Section 1, Section 2 describes the methodology followed to perform the work. Section 3 presents the problem definition, exposing the parameters studied and used to obtain the fitted expressions. Section 4 shows the main results and the proposed fitted expressions. Finally, the main conclusions drawn from this work are presented in Section 5.

2. Methodology

This section describes the methodology followed to compute the vertical and rocking group impedances and the procedure to obtain the fitted expressions. First, the interaction factor superposition method (or elastic superposition method) is explained (Section 2.1), then, the curve fitting procedure is described (Section 2.2).

2.1. The interaction factor superposition method

The vertical and rocking group impedances are obtained by superimposing the vertical interaction effects between all possible pile pairs of the group. Thus, it is possible to determine the dynamic stiffness of a pile group composed of N identical piles by knowing the dynamic stiffness or flexibility of a single and pair of piles at each frequency ω. This simplified method implies that the rest of piles are not influencing the interplay between pile pairs, a simplification very close to reality taking into account that jacket pile group configurations are composed of few piles with large separations.

Applying superposition of effects based on elastic theory, the flexibility and stiffness of a pile group (with identical piles) can be obtained through the sum of two simple submodels, as it is shown in Fig. 1. Submodel (a) corresponds to a single isolated pile subjected to a dynamic vertical load at its head (Q); whereas submodel (b) presents a pile pair separated by a distance S, in which the pile i is the active, source or loaded pile, while pile j is the passive, receiver or unloaded pile. From submodel (a) the vertical displacement of the isolated source pile subjected to its own axial load is calculated (w_{ii}). From submodel (b) the vertical displacement of the receiver pile due to the load acting over the active pile is obtained (w_{ji}). Thus, the vertical flexibility of the source pile (F_{ii}, subproblem (a)) and the flexibility of the receiver pile (F_{ji}, subproblem (b)) can be determined as the relation between the vertical displacement of the source and receiver piles and the axial load respectively (see Eqs. (1) and (2)). These displacements and flexibilities are frequency dependent and complex-valued terms.

$$F_{ii}(\omega) = \frac{w_{ii}(\omega)}{Q(\omega)} \tag{1}$$

$$F_{ji}(\omega) = \frac{w_{ji}(\omega)}{Q(\omega)} \tag{2}$$

The displacements of the source and receiver piles at their heads are computed through a previously developed continuum numerical model [8], particularly developed to efficiently analyse the harmonic behaviour of pile foundations in soils which can be stratified. The model is based on the integral expression of the reciprocity theorem in elastodynamics and the use of effective fundamental solutions to simulate the layered soil behaviour, which already satisfy the interlayer and free-field boundary conditions. This formulation allows to directly consider the radiation damping in the soil region without the need of including any artificial boundary condition. Piles are modelled

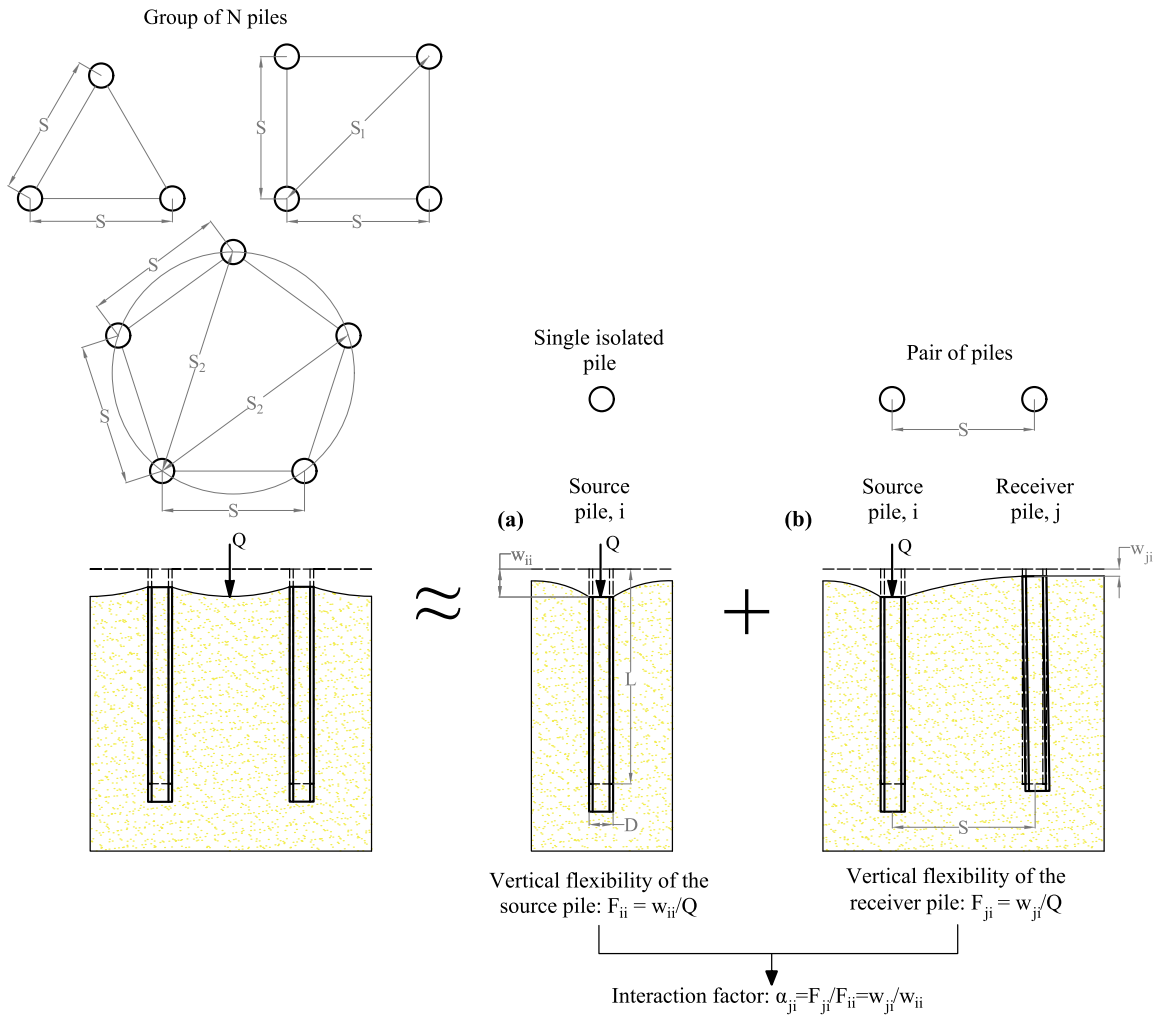

Fig. 1. Vertical modelling approach based on elastic superposition.

as load lines in the soil formulation and as beam finite elements to reproduce their stiffness and inertial contribution. Pile–soil coupling is made by imposing compatibility and equilibrium conditions in terms of displacements and soil–pile interaction forces. Linear-elastic behaviour of soil and piles is assumed. The capacity of this model to correctly reproduce the dynamic behaviour of OWT's foundation elements has been shown in [26].

Once the flexibilities of the source and receiver piles are obtained, the vertical dynamic interaction factor (α_{ji}) can be computed from:

$$\alpha_{ji}(\omega) = \frac{F_{ji}(\omega)}{F_{ii}(\omega)} = \frac{w_{ji}(\omega)}{w_{ii}(\omega)} \tag{3}$$

therefore, knowing this vertical dynamic interaction factor and the flexibility of the source pile, the flexibility of the receiver pile can be expressed in terms of this interaction factor ($F_{ji} = F_{ii}\alpha_{ji}$).

2.1.1. Vertical group impedances calculation

Once the flexibilities of the source pile and the interaction factors are obtained, the vertical flexibility of any pile i of the group (F_i) can be estimated by superimposing the vertical flexibility of the source pile (F_{ii}) with the interaction factors due to its all surrounding piles:

$$F_i = F_{ii}(1 + \sum_{j\neq i}^{j=N} \alpha_{ji}) \tag{4}$$

where N is the number of piles of the group, and α_{ji} is the interaction factor between pile j and i. In this case, as the pile groups are N-sided polygonal configurations, each pile of the group have the same vertical flexibility, so it is enough to determine the vertical flexibility of a unique pile. With this pile vertical flexibility, the pile vertical stiffness (K_i) can be calculated as its inverse:

$$K_i = F_i^{-1} \tag{5}$$

and the vertical group stiffness (K_G) is determined by multiplying it by the number of piles of the group:

$$K_G = N K_i \tag{6}$$

2.1.2. Rocking group impedances calculation due to the vertical component

If a group of piles is subjected at its centre of gravity to a rotation (θ) on the x-axis (as it is described in Fig. 2), it is possible to calculate the vertical displacement that each pile experiences due to this rocking motion as:

$$w_{\theta i} = \theta d_i \tag{7}$$

being d_i the distance between the centre of the pile and the centre of gravity of the group, measured in the y-axis (see Fig. 2). Thus, by using the flexibility definition, it is possible to determine the vertical force that appears at each pile head due to the rocking:

$$Q_{\theta i} = \frac{w_{\theta i}}{F_{\theta i}} \tag{8}$$

where $F_{\theta i}$ is the rocking flexibility due to the vertical component of pile i of the group. This flexibility can be computed with the vertical flexibility of the source pile and the vertical interaction factor:

$$F_{\theta i} = F_{ii}(1 + \sum_{j\neq i}^{j=N} \alpha_{ji} \frac{d_j}{d_i}) \tag{9}$$

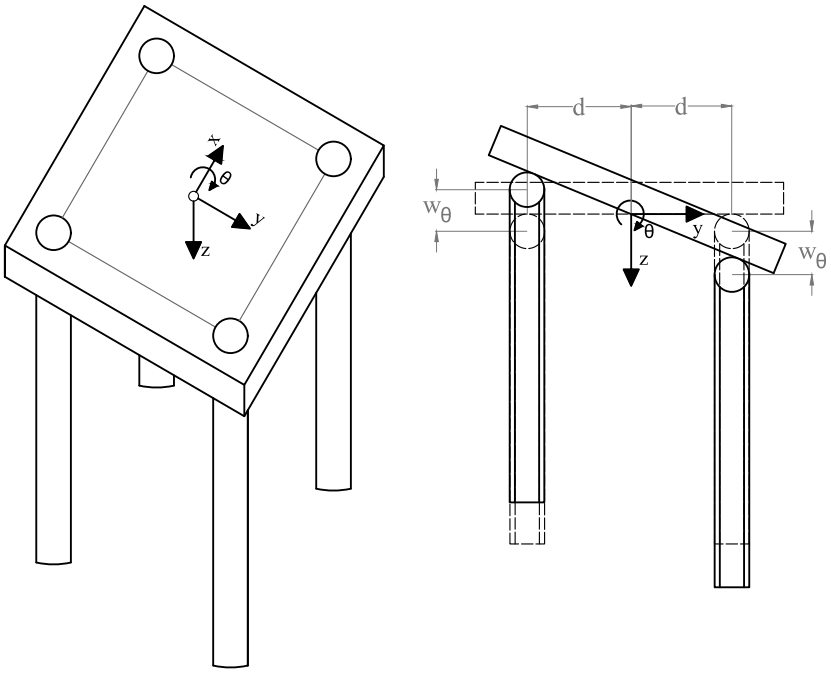

Fig. 2. Rocking problem definition.

being d_j the distance (either positive or negative) between the centre of the adjacent pile (j) and the centre of gravity of the group measured in the y-axis. Thus, for a unitary rotation, replacing Eq. (7) in Eq. (8), and multiplying this by the distance between the pile and the centre of gravity, the contribution of pile i to the group rocking stiffness is determined. In this way, by superimposing the contribution of each pile, the rocking impedance of the group is obtained as:

$$K_{\theta G} = \sum_{i=1}^{i=N} \frac{d_i^2}{F_{\theta i}} \tag{10}$$

This procedure is illustrated assuming a rotation around the x-axis. However, this type of regular polygonal pile arrangements presents an axisymmetric behaviour. Thus, the expressions can be applied to rotations around any axis contained in the xy-plane.

2.2. Proposed expressions for the estimation of the vertical flexibilities of the source pile and interaction factors

The dynamic problem under study depends on many parameters, such as the frequency and pile and soil properties. In this work the variables are defined in dimensionless form. These are: the dimensionless frequency (a_o), which is obtained from:

$$a_o = \frac{\omega D}{V_s} \tag{11}$$

where ω is the frequency, V_s the shear wave velocity of the soil and D the pile diameter; the ratio between the separation among two piles (S) and the diameter (pile spacing ratio: S/D); the relation between the pile length (L) and the pile diameter (pile slenderness ratio: L/D); the ratio between the pile and soil Young's Modulus (Young's Modulus pile–soil ratio: E_p/E_s); the relation between the pile and soil density (density pile–soil ratio: ρ_p/ρ_s); the pile and soil Poisson's ratios (ν_p and ν_s); and the soil hysteretic damping (ξ_s). Among these parameters, the dependency of the dimensionless frequency, pile spacing ratio, pile slenderness relationship, Young's Modulus pile–soil ratio, and soil hysteretic damping is studied on the vertical flexibilities of the source pile, interaction factors and the dynamic group impedances. From these parameters and for a wide and realistic range of them, simple expressions for the estimation of the flexibility of the source pile and interaction factor are fitted through the results computed with the continuum model [8].

In order to obtain expressions that collect the dependency of the main parameters studied, the fits are addressed in two steps. First, the flexibilities of the source pile and interaction factors are fitted for a reference case ($\hat{F}_{ii}$ and $\hat{\alpha}_{ji}$) with the same pile geometry and soil characteristics. For this case, the flexibility of the source pile is fitted as a function of the dimensionless frequency ($\hat{F}_{ii}(a_o)$), while the interaction factor is fitted as a function of the dimensionless frequency and pile spacing ratio ($\hat{\alpha}_{ji}(a_o, S/D)$).

Then, with the aim of introducing the dependency of the pile and soil characteristics in the expressions, different correction factors (β) are computed and fitted to adjust the reference case expressions. The correction factors for the flexibility of the source pile and interaction factor (β_F^P and β_α^P) are defined as a ratio between the flexibility of the source pile or interaction factor due to the change of the generic parameter P (F_{ii}^P and α_{ji}^P) and the reference flexibility of the source pile or interaction factor:

$$\beta_F^P(a_o, P) = \frac{F_{ii}^P(a_o, P)}{\hat{F}_{ii}(a_o)} \tag{12}$$

$$\beta_\alpha^P(a_o, P) = \frac{\alpha_{ji}^P(a_o, \frac{S}{D})}{\hat{\alpha}_{ji}(a_o, \frac{S}{D})} \tag{13}$$

These correction factors are fitted as a function of the dimensionless frequency, or the product of this one and the pile spacing ratio, and the parameter that they rectify. Therefore, the complete expressions of the flexibility of the source pile and interaction factor, are made up of as many correction factors as parameters are going to be rectified:

$$F_{ii}(a_o, \frac{L}{D}, \frac{E_p}{E_s}, \xi_s) = \beta_F^{\frac{L}{D}}(a_o, \frac{L}{D})\beta_F^{\frac{E_p}{E_s}}(a_o, \frac{E_p}{E_s})\beta_F^{\xi_s}(a_o, \xi_s)\hat{F}_{ii}(a_o) \tag{14}$$

$$\alpha_{ji}(a_o, \frac{S}{D}, \frac{L}{D}, \frac{E_p}{E_s}, \xi_s) = \beta_\alpha^{\frac{L}{D}}(a_o, \frac{L}{D})\beta_\alpha^{\frac{E_p}{E_s}}(a_o, \frac{E_p}{E_s})\beta_\alpha^{\xi_s}(a_o \frac{S}{D}, \xi_s)\hat{\alpha}_{ji}(a_o, \frac{S}{D}) \tag{15}$$

In this study, three correction factors are fitted to introduce in the expressions the pile slenderness, Young's Modulus ratios and soil damping dependency. Although the flexibility of the source pile can be easily

Table 1
Parameters studied in this work.

Parameter	Notation	Range/Value	Step
Pile spacing ratio	$\frac{S}{D}$	**[3 20]** [3 20]	**0.5** 1, in (3 6) 2, in (6 12) 4, in (12 20)
Pile slenderness ratio	$\frac{L}{D}$	[10 **20**]	1
Young's Modulus pile–soil ratio	$\frac{E_p}{E_s}$	[50 **500**]	50
Soil hysteretic damping [%]	ξ_s	[**1** 10]	0.25, in (1 1.25) 1.25, in (1.25 10)
Dimensionless frequency	a_o	[0.03 0.25]	0.001
Density pile–soil ratio	$\frac{\rho_p}{\rho_s}$	1.2	
Pile Poisson's ratio	ν_p	0.25	
Soil Poisson's ratio	ν_s	0.40	

computed with a simple model (such as the formulation of a Winkler one), in this work, the correction factor expressions for the flexibility of the source pile are also proposed.

As the flexibilities and interaction factors are complex valued, two fits are performed: one for the absolute value and another one for the argument. This option is chosen over directly fitting the real and imaginary components as it leads to simpler expressions. With these expressions it is pursued to be able to estimate the flexibility of the source pile and interaction factors without the need of executing a meticulous model.

All fits are obtained through a classical least squares regression, considering polynomial of a single or multiple variables (up to a maximum degree of 3) and exponential expressions. The goodness of each fit is evaluated with three commonly used goodness metrics: the sum of squares due to error (SSE), the root mean squared error ($RMSE$) and R-squared (R^2). SSE and $RMSE$ focus on the error magnitude, while R^2 provides insight into the explanatory power of the model. To obtain simple expressions, if two types of fits have similar goodness statistics, the one with fewer parameters is selected.

3. Problem definition

Piles are treated as solid hollow cylindrical foundations embedded in an isotropic homogeneous elastic soil halfspace. This study employs dimensionless variables to enhance the generality of the results. Thus, the vertical flexibility of the source pile and the impedance functions are expressed dimensionlessly based on the pile diameter and the pile's Young's Modulus:

$$F_{ii} D E_s \tag{16}$$

$$\frac{K_G}{D E_s} \tag{17}$$

$$\frac{K_{\theta G}}{D^3 E_s} \tag{18}$$

The dimensionless pile and soil parameters studied in this work as well as their corresponding values are presented in Table 1. The first (upper) part of this table shows the different parameters used to carry out the fitting expressions, being the values in bold text those that are used for the reference case, whereas the others for the correction factor (β) fits. The second (bottom) part of the table lists the dimensionless frequency range and the identical parameters adopted for both the reference case and correction factor fits.

Regarding the parameters considered in Table 1, typical geometric values of jacket pile groups are adopted, covering a large range of pile spacing ratios (from 3 to 20) and pile slenderness ratios (from 10 and 20), representing flexible piles which are typical of this type of pile groups. The Young's Modulus ratio interval is chosen from 50 to 500, corresponding to hollow steel piles in medium-to-soft seabeds. This ratio interval is established considering that the pile Young's Modulus is the equivalent of a cylindrical hollow steel pile with soil mass in its inside. For that purpose, a pile thickness (t_p) of 1.30% of the diameter is selected. This value has been obtained following the pile thickness API's recommendation [27] (see Eq. (19)), where a pile thickness of 1.6% and 1.2% is obtained for a pile diameter of 1 m and 3 m respectively. Soil hysteretic damping spans from 1 to 10%, covering the interval between 2 and 5% that is the commonly employed for seabed profiles.

$$t_p \geq 6.35 + \frac{D}{100} \text{ [mm]} \tag{19}$$

Concerning the same parameters that are adopted in all fits (both in the reference case and in the interaction correction factor fits, presented in the second part of Table 1), the dimensionless frequency (a_o) interval considered ranges from 0.03 to 0.25. The upper value corresponds to a diameter equal to a quarter of the wave length, being within the range of application of the beam-soil continuum model. The density pile–soil ratio adopted is the equivalent density of a cylindrical hollow steel pile with soil mass in its inside, considering a pile thickness of 1.30% of the diameter, in coherence with the Young's Modulus ratio interval. Poisson's ratios of 0.40 and 0.25 are selected for the soil and pile accordingly, usual values of sandy and clays seabed profiles and structural steel. A null hysteretic damping coefficient is assumed for the structural steel of the pile.

With respect to the values adopted to obtain the reference fits (indicated in bold text in Table 1), a pile slenderness ratio of 20, Young's Modulus ratio of 500 and soil damping of 1% are chosen. The flexibilities of the source pile and interaction factors for this reference case ($\hat{F}_{ii}$ and $\hat{\alpha}_{ji}$) are fitted by employing a wide range of pile spacing ratios, from 3 to 20 with steps of 0.5. The other values shown are used to obtain the fitting curves of the correction factors for the flexibility of the source pile and interaction factors (β_F^P and β_α^P). As it can be observed, the reference values are the upper (for the pile slenderness and Young's Modulus ratios) or lower limit (for the soil damping) of the considered intervals. In this way, the reference case is a limit configuration from which the others are obtained.

To validate the proposed procedure in terms of group impedances, three pile regular configurations (of 3, 4 and 5 piles) are studied, where each pile is located at each vertex of the polygon (see Fig. 3). All pile groups are assumed to be rigidly connected between them, a properly assumption for pile groups of jacket-supported OWTs. This rigid connection could be a unique structural element or several elements, such as a cap mass or beam framing joining the piles.

4. Results and discussion

With the aim of addressing the proposed objectives, the results presented in this section are organised into two parts: analysis of the reference case and analysis of correction factors.

In Section 4.1 the reference case is studied. First, the proposed fitted reference expressions to compute the vertical flexibilities of the source pile and interaction factors are shown. The vertical flexibility of the source pile and some interaction factors for different pile spacings are represented, comparing the results obtained with the fitted expressions with those directly computed with the continuum model. Then, the dynamic vertical and rocking impedances are analysed for this reference scenario. The impedances directly determined by the rigorous model are compared with those obtained by the interaction factor superposition method. The superposition is applied for the flexibilities and interaction factors directly obtained with the continuum model and with the proposed fitted expressions. In this way, the validity of both the superposition method and the fitted expressions is tested up.

In Section 4.2, the correction factors used to complete and include the dependency of the other parameters within the overall flexibility and interaction factor expressions are presented. First, the dependency

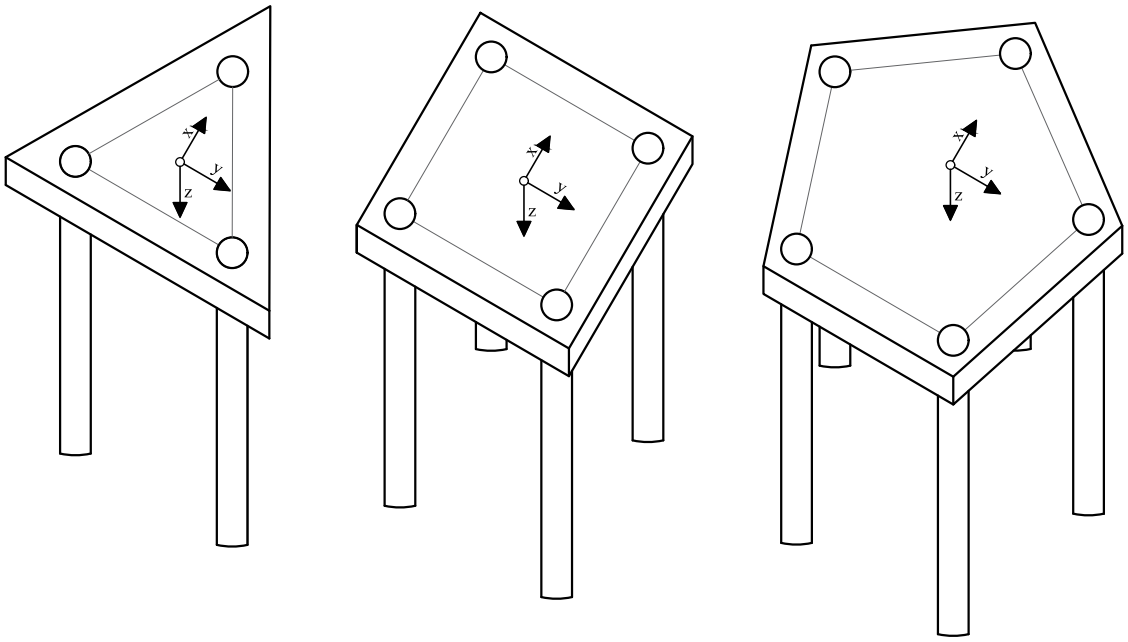

Fig. 3. Polygonal configurations of pile groups for jacket-supported OWTs studied in this work.

of these correction factors is analysed and their proposed fitted expressions are shown. Next, the effect of each correction factor is individually studied, by comparing the vertical and rocking group impedances obtained through the superposition of the fitted expressions, with the superposition of the direct model flexibilities and interaction factors. Afterwards, at the end of this Section 4.2, three cases with different configuration of parameters are studied comparing the model and fitting superposition results in order to analyse the correction as a whole.

4.1. Reference case

4.1.1. Proposed and fitted expressions

The fits obtained for the vertical flexibility of the source pile and interaction factor of the reference case ($L/D = 20$, $E_p/E_s = 500$ and $\xi_s = 1\%$) are exposed in Table 2. For the absolute value and argument of the flexibility of the source pile an exponential and polynomial expression of degree 1 are proposed, whereas for the interaction factor fits a multidegree polynomial expression of degrees 1 and 2 are suggested. The goodness statistics of each fit are also presented in Table 2, being SSE the sum of squares due to error, R^2 the R-squared statistic and $RMSE$ the root mean squared error. As it is exposed, all reference expressions have excellent goodness statistics, since all SSE and $RMSE$ take low values, as well as all R^2 are close to unity. All fits are chosen as a compromise between evaluating their simplicity and the accuracy of their results. For this reference case it is important to obtain expressions with acceptable goodness characteristics, because the complete expressions are based on these reference fits (see Eqs. (14) and (15)).

Fig. 4 shows the dimensionless flexibility of the source pile and the interaction factors for different pile spacing ratios ($S/D = 4, 6$ and 10) against the dimensionless frequency. The dimensionless flexibilities of the source pile are depicted in the first row and the interaction factors in the other ones. The real and imaginary parts are presented in the first and second column respectively. With different colours the results obtained through the fitting expressions (red curves), the model (blue curves) and with the Dobry and Gazetas [11] interaction factor expression (see Eq. (20), green curve) are distinguished. In Eq. (20) the term i refers to the imaginary unit ($\sqrt{-1}$). As it is shown in this equation, the interaction factor proposed by Dobry and Gazetas depends on the pile spacing ratio, the dimensionless frequency and the soil damping. In Fig. 4 it can be seen that the flexibilities of the source pile and interaction factors computed with the proposed fitted expressions align with those directly determined with the continuum model. The interaction factors obtained also matches well with the expression proposed by Dobry and Gazetas, especially for big pile spacing ratios. The flexibility of the source pile shows a slight curved variation over the frequency range, while the interaction factor presents the expected oscillatory behaviour. For the interaction factor, as pile spacing increases the oscillation amplitude and frequency (both in the real and imaginary parts) diminishes. The increase of the pile spacing produces a less interference among piles, as well as soil has more time to deform and dissipate the wave energy, leading to a lower resonant frequency.

$$\alpha_{ji}^{DG} = \left(2\frac{S}{D}\right)^{-\frac{1}{2}} \mathrm{e}^{2\pi a_o \frac{S}{D}(\mathrm{i}-\xi_s)} \tag{20}$$

4.1.2. Vertical and rocking dynamic impedances

In Fig. 5 the dimensionless vertical group impedances (y-axis) for the three, four and five pile groups are shown against the dimensionless frequency (x-axis) for the reference case. Results for each pile configuration are depicted in two columns: the real (stiffness component) and imaginary (damping component) part in the first and second column respectively. Group impedances for different pile spacing ratios ($S/D = 4, 6, 8$ and 10) are arranged by rows. With different colours the results directly obtained through the model (Direct-Model, black curves) are distinguished from those computed applying the superposition method. With a blue and red curve the impedances obtained by superimposing the flexibilities and interaction factors determined through the model ($\hat{\mathrm{F}}, \hat{\alpha}$-Model) and the fitted expressions ($\hat{\mathrm{F}}, \hat{\alpha}$-Fitting) are shown, while with a green curve the results computed by elastic superposition using the model flexibilities of the source pile and Dobry and Gazetas interaction factors (Eq. (20)) are represented. Following the same distribution, Fig. 6 shows the dimensionless rocking group impedances.

It can be observed that the impedances obtained through the interaction factor superposition method are generally similar to those directly computed through the model, both in the vertical and rocking impedances. For the vertical group impedances (Fig. 5) and the lowest pile separation ratio ($S/D = 4$), it can be appreciated a phase difference between the direct model maximum results and the maximum obtained

Table 2
Fitted expressions of the reference case.

Fitted expression/Type	Fitting parameters		Fitting characteristics	
$\mathrm{Abs}(\hat{F}_{ii}(a_o)) = \mathrm{a}e^{\mathrm{b}a_o}\frac{1}{DE_s}$	a	$7.96 \cdot 10^{-2}$	SSE	$4.86 \cdot 10^{-4}$
	b	-3.35	R^2	$9.81 \cdot 10^{-1}$
Exponential of 1 degree			$RMSE$	$1.50 \cdot 10^{-3}$
$\mathrm{Arg}(\hat{F}_{ii}(a_o)) = \mathrm{p}_1 a_o + \mathrm{p}_2$	p_1	-2.71	SSE	$4.42 \cdot 10^{-2}$
	p_2	$-4.01 \cdot 10^{-1}$	R^2	$9.93 \cdot 10^{-1}$
Linear regression			$RMSE$	$1.42 \cdot 10^{-2}$
$\mathrm{Abs}(\hat{\alpha}_{ji}(a_o, \frac{S}{D})) = \mathrm{p}_{00} + \mathrm{p}_{10}a_o + \mathrm{p}_{01}\frac{S}{D} + \mathrm{p}_{11}a_o\frac{S}{D} + \mathrm{p}_{02}\left(\frac{S}{D}\right)^2$	p_{00}	$4.20 \cdot 10^{-1}$	SSE	$6.13 \cdot 10^{-1}$
	p_{10}	$-1.96 \cdot 10^{-1}$	R^2	$9.79 \cdot 10^{-1}$
	p_{01}	$-2.89 \cdot 10^{-2}$	$RMSE$	$8.90 \cdot 10^{-3}$
	p_{11}	$-1.40 \cdot 10^{-3}$		
Multivariate polynomial of 1 and 2 degrees	p_{02}	$7.72 \cdot 10^{-4}$		
$\mathrm{Arg}(\hat{\alpha}_{ji}(a_o, \frac{S}{D})) = \mathrm{p}_{00} + \mathrm{p}_{10}a_o + \mathrm{p}_{01}\frac{S}{D} + \mathrm{p}_{11}a_o\frac{S}{D} + \mathrm{p}_{02}\left(\frac{S}{D}\right)^2$	p_{00}	$-1.02 \cdot 10^{-1}$	SSE	1.39
	p_{10}	1.34	R^2	1
	p_{01}	$-2.51 \cdot 10^{-2}$	$RMSE$	$1.34 \cdot 10^{-2}$
	p_{11}	-6.29		
Multivariate polynomial of 1 and 2 degrees	p_{02}	$1.14 \cdot 10^{-4}$		

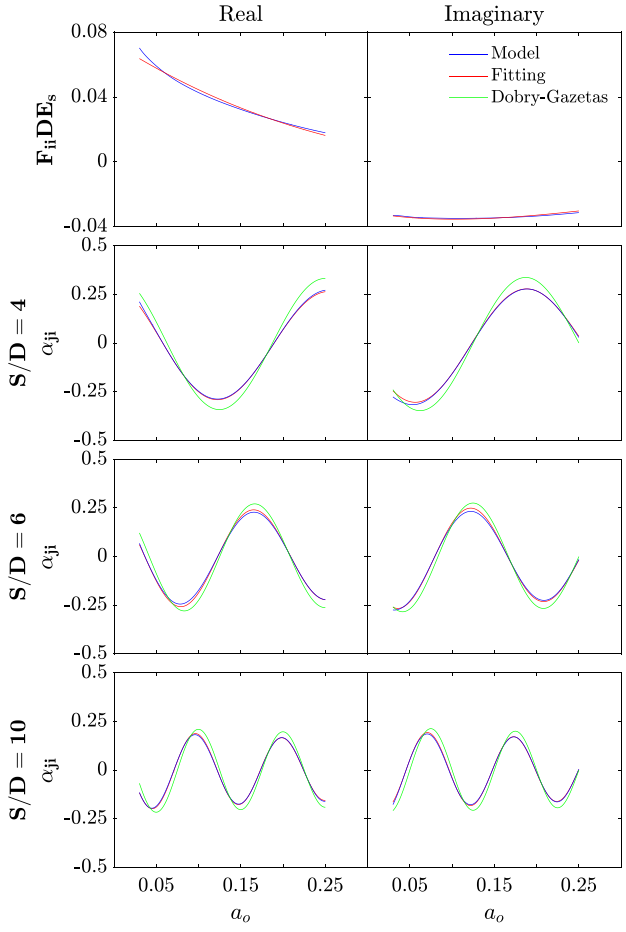

Fig. 4. Flexibility of the source pile and interaction factor for the reference case. (For interpretation of the references to colour in this figure legend, the reader is referred to the web version of this article.)

through the superposition method of the model and fitted flexibilities of the source pile and interaction factor. This maximum occurs at lightly higher frequencies when the interaction between all piles of the group is considered (Direct-Model results). This effect is due to the scattering of waves produced by the presence of all piles, which is only considered in the direct-model results (black curve). This occurs to a greater extent for the smallest pile spacing ($S/D = 4$), while for larger pile spacings this phase difference tends to decrease (note that for the $S/D = 6$ this phase difference practically does not exist). In this way, it is verified that the adjacent piles to the pile pair do not significantly affect the interplay between the pair for wavelengths larger than six times the pile diameter, assumption that was already established in [11]. Despite this difference between the vertical dynamic impedances obtained through the direct model and those of the interaction factor superposition method given for the $S/D = 4$, results computed by superposition reproduce quite well the impedance functions over the entire frequency range. Thus, for this type foundations, with large pile spacing ratios ($S/D \geq 4$), the interaction factor superposition can be employed to compute accurately enough the vertical and rocking impedance functions. The vertical impedances got with the superposition of the Dobry and Gazetas interaction factors show differences with respect to the fitting and model impedances. These differences are mainly appreciated at the impedance peaks, in which a phase and a magnitude difference are produced, conducting to greater peaks. Such peak differences are reduced as the number of piles of the group decreases and the pile spacing ratio increases. Regarding the rocking group stiffnesses and dampings (Fig. 6), the impedances determined through the fitted interaction factors and flexibilities of the source pile match well with the ones obtained through the continuum model. Only some discrepancies can be found at very low or high frequencies. In this case, the differences of the rocking impedances computed with the Dobry and Gazetas interaction factors with respect to the fitting and model results are lower than those given in the vertical impedances. As it was expected, both in the vertical and rocking impedances, a more pronounced group behaviour is observed with the increase of the number of piles. Increasing pile separation ratio produces a reduction in the vertical impedances and a growth of the rocking ones. Furthermore, with the increase of the pile spacing, more number of peaks appears in both the vertical and rocking impedances. Note that for a same frequency range more multiples of the wavelength fit within a greater pile separation. A similar trend is observed when the number of piles increases for the rocking impedances, producing more number of peaks. All these last comments agree well with the conclusions of the classical works (such as [4]). It is worth noting that, for comparison purposes, the rocking impedance functions obtained through the direct continuum model are computed assuming a pile group with hinged heads. This assumption is made to completely remove any contribution of the lateral mode of the piles. However, for the studied configurations, the rocking impedance of the group is mainly governed by the axial stiffness of the piles and, therefore, the results can be extended to groups with rotationally fixed pile heads.

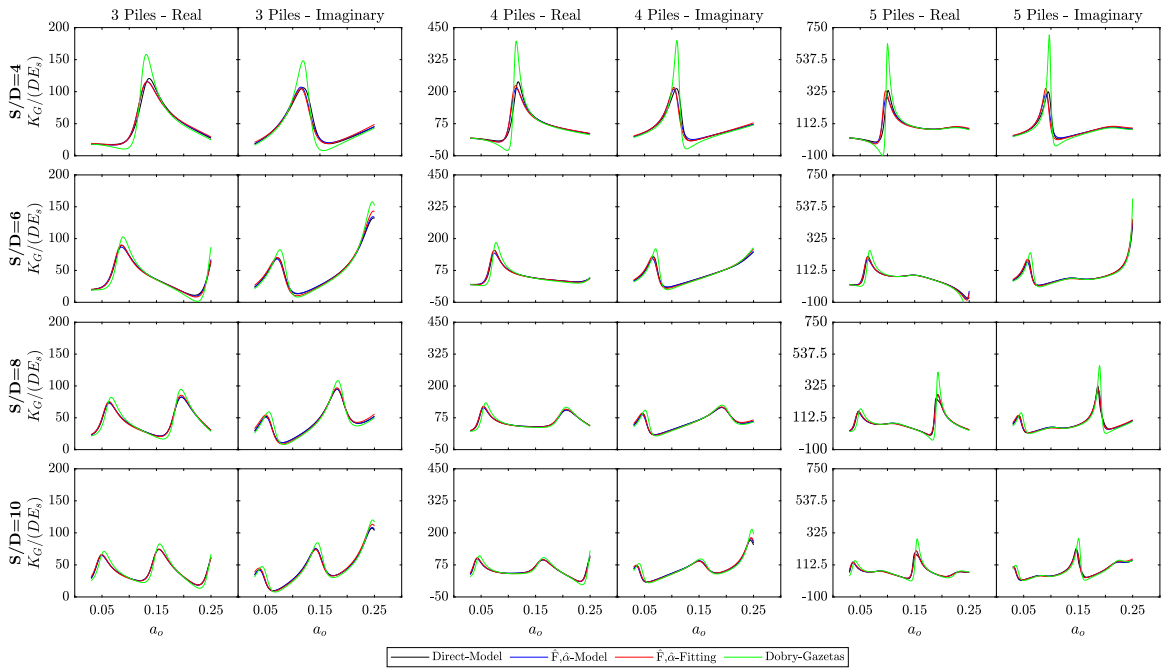

Fig. 5. Vertical group impedances for the reference case. (For interpretation of the references to colour in this figure legend, the reader is referred to the web version of this article.)

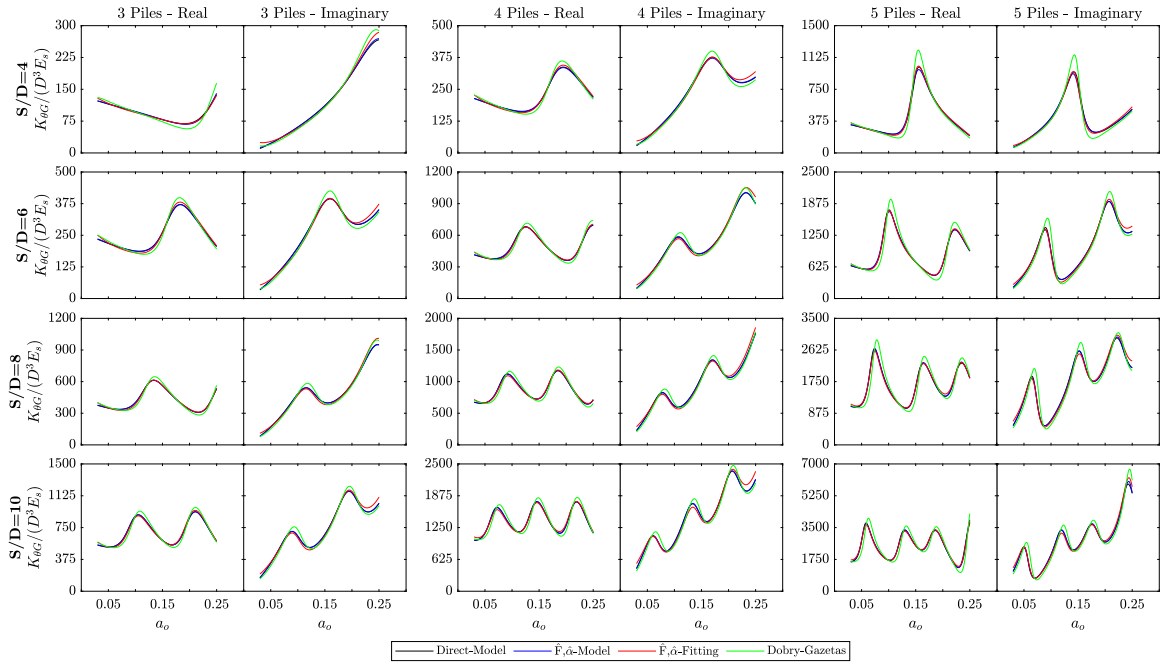

Fig. 6. Rocking group impedances for the reference case. (For interpretation of the references to colour in this figure legend, the reader is referred to the web version of this article.)

4.2. Inclusion of correction factors

As previously mentioned in Section 2.2, with the aim of including the dependency of more parameters in the expressions, some correction factors are also fitted to adjust the reference case expressions. To fulfil this objective, firstly, the influence of the pile slenderness, Young's Modulus ratios and the soil damping is studied for each correction factor. Once this influence is analysed, it is studied how well this correction factor reproduces the variation due to each parameter.

4.2.1. Correction factors for the vertical flexibilities of the source pile

To analyse the flexibilities of the source pile variation with respect to the reference case when some of the system parameters change, Fig. 7 represents the correction factor for the flexibility of the source pile (β_F) against the dimensionless frequency. Each row shows these correction factors for each analysed parameter: the pile slenderness ratio, the Young's Modulus pile–soil ratio and the soil damping. The real and imaginary components of these correction factors are presented in columns. Different colours are used to show the correction factors for diverse values of each parameter. In Fig. 7 it can be observed that the pile slenderness and the Young's Modulus ratios, have a remarkable

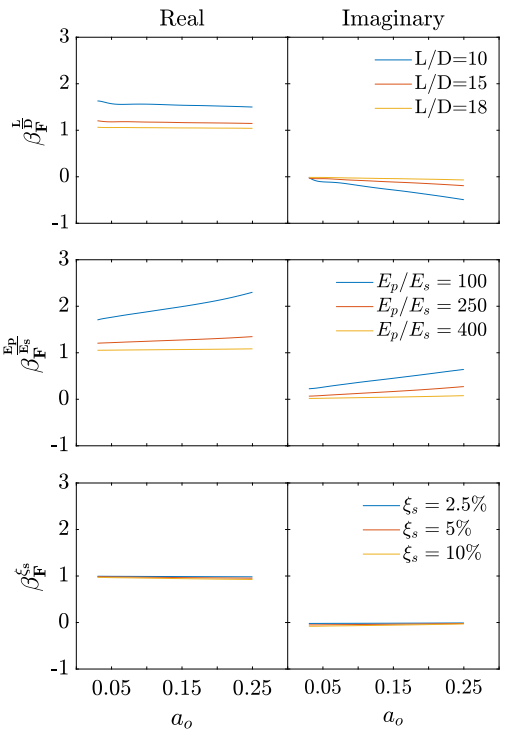

Fig. 7. Correction factors for the flexibility of the source pile against dimensionless frequency. (For interpretation of the references to colour in this figure legend, the reader is referred to the web version of this article.)

influence on the flexibility of the source pile as the results differ from those obtained for the reference case ($L/D = 20$ and $E_p/E_s = 500$). In terms of the soil damping there are no significant differences with respect to the reference case, both in the real and imaginary components. As regards the pile slenderness ratio influence, it can be seen that lower pile slenderness increases the flexibility, as the pile–soil interaction surface decreases. This is because the influence of the pile length on the dimensionless vertical dynamic flexibility of the pile is larger than that of the pile diameter. Besides, a phase difference is produced for low pile lengths as the frequency increases. Respecting the Young's Modulus ratio, low values (less pile stiffness with respect to the soil one) imply higher flexibilities and phase differences in the entire frequency range.

In Table 3 the correction factor fits for the flexibilities of the source pile are presented. The expressions are fitted in terms of the dimensionless frequency and the parameter that each correction factor adjusts. All fits are multivariate polynomial expressions of degrees 1 and 2 (for the pile slenderness ratio and soil damping correction factors) and 1 and 3 (for the Young's Modulus pile–soil correction factor). According to the metrics presented in Table 3, all fitted expressions present a high level of accuracy for reproducing the model's results. Although the variation of the correction factor for the flexibility of the source pile in terms of the soil damping is very small (see Fig. 7), this correction factor is also fitted, since the assumption of not rectifying the flexibility of the source pile with the variation of this parameter affects in a significantly way the results when the soil damping is greater than 5% (this fact will be shown and commented in Section 4.2). All expressions are obtained evaluating their simplicity and accuracy of the fits.

4.2.2. Interaction correction factors

In Fig. 8 the interaction correction factor for each parameter P is presented versus the dimensionless frequency. The interaction correction factors for the pile slenderness ratio are depicted in the firsts two columns (real and imaginary part), in which the results corresponding to a ratio of 10, 15 and 18 are arranged in the first, second and third rows respectively. In the following two columns the interaction correction factors for the Young's Modulus ratio are shown, for values of 100, 250 and 400 in each row. Finally, the interaction correction factors corresponding to the soil damping are represented in the last two columns, for soil dampings of 2.5, 5 and 7.5%. Different colours are used to distinguish the correction factors for different pile spacing ratios. In Fig. 8 it can be observed that the interaction correction factors for the pile slenderness, Young's Modulus ratios and soil dampings, show a considerable dependency of the dimensionless frequency and pile spacing ratio, except for large pile slenderness and Young's Modulus ratios and the imaginary component of pile damping correction factor. Furthermore, the variation of the soil damping interaction correction factor with the dimensionless frequency and the pile separation is uniform, however, for the pile slenderness and Young's Modulus ratios it is not. This fact can be seen for the smaller values of the pile slenderness and Young's Modulus ratios, where the variation of the interaction correction factor is not uniform with the frequency, above all for larger pile spacing ratios.

In Table 4 the fitted expressions obtained for the interaction correction factor of each parameter are shown. On the one hand, the correction factors for the pile slenderness and Young's Modulus ratios are fitted in terms of the dimensionless frequency and the parameter that is rectified. The pile spacing dependency is not directly included as a variable in theses expressions, but it is implicitly within them, because the results corresponding to each pile spacing are used to obtain the expressions. On the other hand, the soil damping correction factor is fitted in terms of the product of the dimensionless frequency and pile spacing ratio, and the soil damping. Thus, the dimensionless frequency, pile spacing ratio and soil damping dependency is explicitly reproduced within the soil damping interaction correction factor. The expressions of the pile slenderness and Young's Modulus correction factors were also attempted to be fitted in terms of this product, but they led to worse results. All fits are multivariate polynomial functions of up 2 degrees. However, the arguments of the interaction correction factor for the Young's Modulus ratio and soil damping are not considered, since their fittings turned out to give superficial functions very close to zero, so this assumption allows to simplify the expressions leading to similar results. The characteristics of these fits are inferior to those described previously (reference case and correction factor fits for the flexibilities of the source pile, Tables 2 and 3), especially for the pile slenderness and Young's Modulus ratios, because the pile spacing dependency is not directly reproduced in these expressions.

4.2.3. Vertical and rocking impedances

In order to analyse how these correction factors (both for the flexibility of the source pile and interaction factor) allow to adjust the reference case, this section is organised as follows: Firstly, it is studied how each correction factor fixes the variation of its respective parameter, this is done by only varying the parameter that is analysed maintaining the others with the reference case values; finally, some cases in which all parameters are modified at the same time are analysed. For simplification purpose, only the results corresponding to the 4-pile group are shown, for the 3 and 5-pile groups, similar conclusions are obtained.

– **Influence of pile slenderness ratio**

Fig. 9 shows the dimensionless vertical impedances of a 4-pile group for different pile spacing ($S/D = 4, 6, 8$ and 10) and pile slenderness ratios ($L/D = 10, 15$ and 18) against the dimensionless frequency. In these results only the pile slenderness and pile spacing ratios are varied, all other parameters are kept invariant adopting the values of the reference case ($E_p/E_s = 500$ and $\xi_s = 1\%$). Results for each pile spacing and pile slenderness ratio are arranged by rows and pair of columns respectively. At the first column of each pair the real component is presented while in the second one the imaginary part. With different

Table 3
Fitted expressions of the correction factors for the flexibilities of the source pile.

Fitted expression	Fitting parameters		Fitting characteristics	
$\mathrm{Abs}(\beta_F^{\frac{L}{D}}(a_o,\frac{L}{D})) = \mathrm{p}_{00} + \mathrm{p}_{10}a_o + \mathrm{p}_{01}\frac{L}{D} + \mathrm{p}_{11}a_o\frac{L}{D} + \mathrm{p}_{02}\left(\frac{L}{D}\right)^2$	p_{00}	3.05	SSE	$1.98\cdot10^{-1}$
	p_{10}	$-1.91\cdot10^{-1}$	R^2	$9.98\cdot10^{-1}$
	p_{01}	$-1.93\cdot10^{-1}$	$RMSE$	$9.00\cdot10^{-3}$
	p_{11}	$6.55\cdot10^{-3}$		
Multivariate polynomial of 1 and 2 degrees	p_{02}	$4.55\cdot10^{-3}$		
$\mathrm{Arg}(\beta_F^{\frac{L}{D}}(a_o,\frac{L}{D})) = \mathrm{p}_{00} + \mathrm{p}_{10}a_o + \mathrm{p}_{01}\frac{L}{D} + \mathrm{p}_{11}a_o\frac{L}{D} + \mathrm{p}_{02}\left(\frac{L}{D}\right)^2$	p_{00}	$5.48\cdot10^{-2}$	SSE	$1.89\cdot10^{-2}$
	p_{10}	-2.54	R^2	$9.99\cdot10^{-1}$
	p_{01}	$-7.26\cdot10^{-3}$	$RMSE$	$2.80\cdot10^{-3}$
	p_{11}	$1.27\cdot10^{-1}$		
Multivariate polynomial of 1 and 2 degrees	p_{02}	$2.26\cdot10^{-4}$		
$\mathrm{Abs}(\beta_F^{\frac{E_p}{E_s}}(a_o,\frac{E_p}{E_s})) = \mathrm{p}_{00} + \mathrm{p}_{10}a_o + \mathrm{p}_{01}\frac{E_p}{E_s} + \mathrm{p}_{11}a_o\frac{E_p}{E_s} + \mathrm{p}_{02}\left(\frac{E_p}{E_s}\right)^2 + \mathrm{p}_{12}a_o\left(\frac{E_p}{E_s}\right)^2 + \mathrm{p}_{03}\left(\frac{E_p}{E_s}\right)^3$	p_{00}	2.98	SSE	7.49
	p_{10}	5.50	R^2	$9.90\cdot10^{-1}$
	p_{01}	$-1.75\cdot10^{-2}$	$RMSE$	$5.83\cdot10^{-2}$
	p_{11}	$-2.76\cdot10^{-2}$		
	p_{02}	$5.39\cdot10^{-5}$		
	p_{12}	$3.42\cdot10^{-5}$		
Multivariate polynomial of 1 and 3 degrees	p_{03}	$-5.42\cdot10^{-8}$		
$\mathrm{Arg}(\beta_F^{\frac{E_p}{E_s}}(a_o,\frac{E_p}{E_s})) = \mathrm{p}_{00} + \mathrm{p}_{10}a_o + \mathrm{p}_{01}\frac{E_p}{E_s} + \mathrm{p}_{11}a_o\frac{E_p}{E_s} + \mathrm{p}_{02}\left(\frac{E_p}{E_s}\right)^2 + \mathrm{p}_{12}a_o\left(\frac{E_p}{E_s}\right)^2 + \mathrm{p}_{03}\left(\frac{E_p}{E_s}\right)^3$	p_{00}	$1.82\cdot10^{-1}$	SSE	$1.05\cdot10^{-1}$
	p_{10}	$3.21\cdot10^{-1}$	R^2	$9.93\cdot10^{-1}$
	p_{01}	$-4.78\cdot10^{-4}$	$RMSE$	$6.90\cdot10^{-3}$
	p_{11}	$3.41\cdot10^{-3}$		
	p_{02}	$-1.07\cdot10^{-6}$		
	p_{12}	$-8.52\cdot10^{-6}$		
Multivariate polynomial of 1 and 3 degrees	p_{03}	$2.73\cdot10^{-9}$		
$\mathrm{Abs}(\beta_F^{\xi_s}(a_o,\xi_s)) = \mathrm{p}_{00} + \mathrm{p}_{10}a_o + \mathrm{p}_{01}\xi_s + \mathrm{p}_{11}a_o\xi_s + \mathrm{p}_{02}\xi_s^2$	p_{00}	1.00	SSE	$9.87\cdot10^{-4}$
	p_{10}	$2.48\cdot10^{-2}$	R^2	$9.99\cdot10^{-1}$
	p_{01}	$-3.02\cdot10^{-3}$	$RMSE$	$7.05\cdot10^{-4}$
	p_{11}	$-3.22\cdot10^{-2}$		
Multivariate polynomial of 1 and 2 degrees	p_{02}	$-4.85\cdot10^{-5}$		
$\mathrm{Arg}(\beta_F^{\xi_s}(a_o,\xi_s)) = \mathrm{p}_{00} + \mathrm{p}_{10}a_o + \mathrm{p}_{01}\xi_s + \mathrm{p}_{11}a_o\xi_s + \mathrm{p}_{02}\xi_s^2$	p_{00}	$1.61\cdot10^{-2}$	SSE	$2.40\cdot10^{-3}$
	p_{10}	$-4.14\cdot10^{-2}$	R^2	$9.99\cdot10^{-1}$
	p_{01}	$-1.54\cdot10^{-2}$	$RMSE$	$1.10\cdot10^{-3}$
	p_{11}	$3.56\cdot10^{-2}$		
Multivariate polynomial of 1 and 2 degrees	p_{02}	$1.33\cdot10^{-4}$		

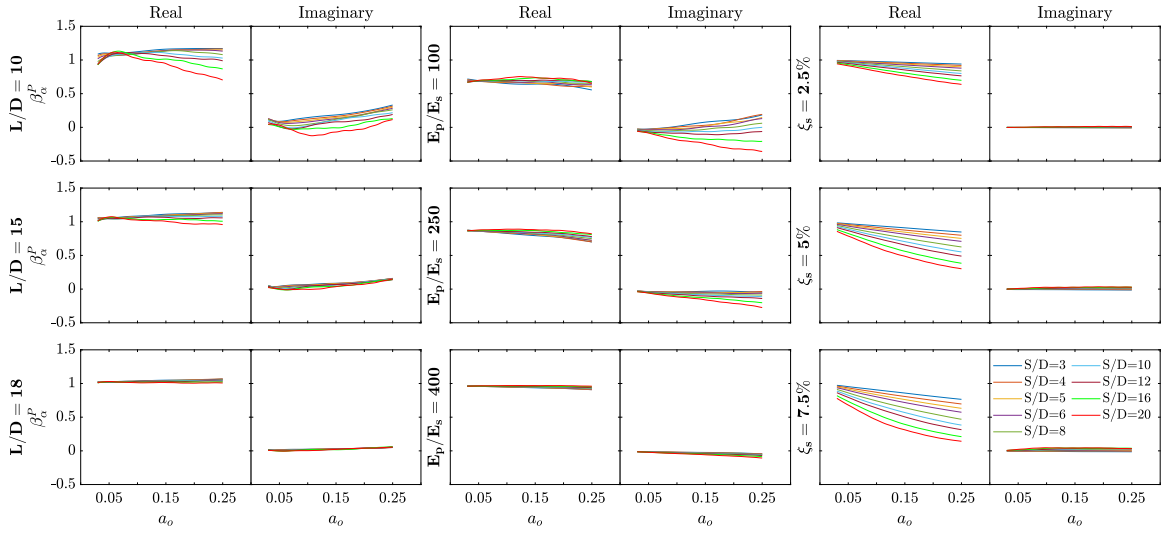

Fig. 8. Interaction correction factors against dimensionless frequency. (For interpretation of the references to colour in this figure legend, the reader is referred to the web version of this article.)

colours the following curves are presented: the impedances obtained through superposition of the flexibilities and interaction factors of the fitted expressions (red curve, F, α-Fitting); those computed by using the flexibilities and interaction factors of the model (blue curve, F, α-Model); the reference case impedances determined with their corresponding fits (green dashed curve, $\hat{\mathrm{F}}$, $\hat{\alpha}$-Fitting); and the impedances got by superimposing the fitted flexibilities of the source pile (adjusted through their correction factors) with the fitted interaction factors of the reference case (cyan dashed curve, F, $\hat{\alpha}$-Fitting). In Fig. 9 it can be observed that the impedances computed through the fitted interaction factors and flexibilities of the source pile agree well with the model ones. The biggest differences between these occur at the first peak of the impedances (both in the real and imaginary parts), in which the fitting peak is above of the model one (except the case with the

Table 4
Fitted expressions of the interaction correction factors.

Fitted expression	Fitting parameters		Fitting characteristics	
$\mathrm{Abs}(\beta_\alpha^{\frac{L}{D}}(a_o, \frac{L}{D})) = \mathrm{p}_{00} + \mathrm{p}_{10}a_o + \mathrm{p}_{01}\frac{L}{D} + \mathrm{p}_{11}a_o\frac{L}{D} + \mathrm{p}_{02}\left(\frac{L}{D}\right)^2$	p_{00}	$9.21 \cdot 10^{-1}$	SSE	$5.06 \cdot 10$
	p_{10}	$9.45 \cdot 10^{-2}$	R^2	$2.75 \cdot 10^{-1}$
	p_{01}	$2.64 \cdot 10^{-2}$	$RMSE$	$4.81 \cdot 10^{-2}$
	p_{11}	$1.37 \cdot 10^{-3}$		
Multivariate polynomial of 1 and 2 degrees	p_{02}	$-1.17 \cdot 10^{-3}$		
$\mathrm{Arg}(\beta_\alpha^{\frac{L}{D}}(a_o, \frac{L}{D})) = \mathrm{p}_{00} + \mathrm{p}_{10}a_o + \mathrm{p}_{01}\frac{L}{D} + \mathrm{p}_{20}a_o^2 + \mathrm{p}_{11}a_o\frac{L}{D}$	p_{00}	$2.23 \cdot 10^{-3}$	SSE	$1.95 \cdot 10$
	p_{10}	1.01	R^2	$7.15 \cdot 10^{-1}$
	p_{01}	$1.85 \cdot 10^{-3}$	$RMSE$	$2.98 \cdot 10^{-2}$
	p_{20}	2.54		
Multivariate polynomial of 2 and 1 degrees	p_{11}	$-8.35 \cdot 10^{-2}$		
$\mathrm{Abs}(\beta_\alpha^{\frac{E_p}{E_s}}(a_o, \frac{E_p}{E_s})) = \mathrm{p}_{00} + \mathrm{p}_{10}a_o + \mathrm{p}_{01}\frac{E_p}{E_s} + \mathrm{p}_{11}a_o\frac{E_p}{E_s} + \mathrm{p}_{02}\left(\frac{E_p}{E_s}\right)^2$	p_{00}	$6.11 \cdot 10^{-1}$	SSE	$3.08 \cdot 10$
	p_{10}	$-1.23 \cdot 10^{-2}$	R^2	$8.93 \cdot 10^{-1}$
	p_{01}	$1.03 \cdot 10^{-3}$	$RMSE$	$3.94 \cdot 10^{-2}$
	p_{11}	$-5.04 \cdot 10^{-4}$		
Multivariate polynomial of 1 and 2 degrees	p_{02}	$-3.12 \cdot 10^{-7}$		
$\mathrm{Arg}(\beta_\alpha^{\frac{E_p}{E_s}}(a_o, \frac{E_p}{E_s})) = 0$				
$\mathrm{Abs}(\beta_\alpha^{\xi_s}(a_o\frac{S}{D}, \xi_s)) = \mathrm{p}_{00} + \mathrm{p}_{10}a_o\frac{S}{D} + \mathrm{p}_{01}\xi_s + \mathrm{p}_{20}(a_o\frac{S}{D})^2 + \mathrm{p}_{11}a_o\frac{S}{D}\xi_s$	p_{00}	1.08	SSE	$2.71 \cdot 10$
	p_{10}	$-8.54 \cdot 10^{-2}$	R^2	$9.68 \cdot 10^{-1}$
	p_{01}	$-1.66 \cdot 10^{-2}$	$RMSE$	$3.89 \cdot 10^{-2}$
	p_{20}	$1.98 \cdot 10^{-2}$		
Multivariate polynomial of 2 and 1 degrees	p_{11}	$-2.41 \cdot 10^{-2}$		
$\mathrm{Arg}(\beta_\alpha^{\xi_s}(a_o\frac{S}{D}, \xi_s)) = 0$				

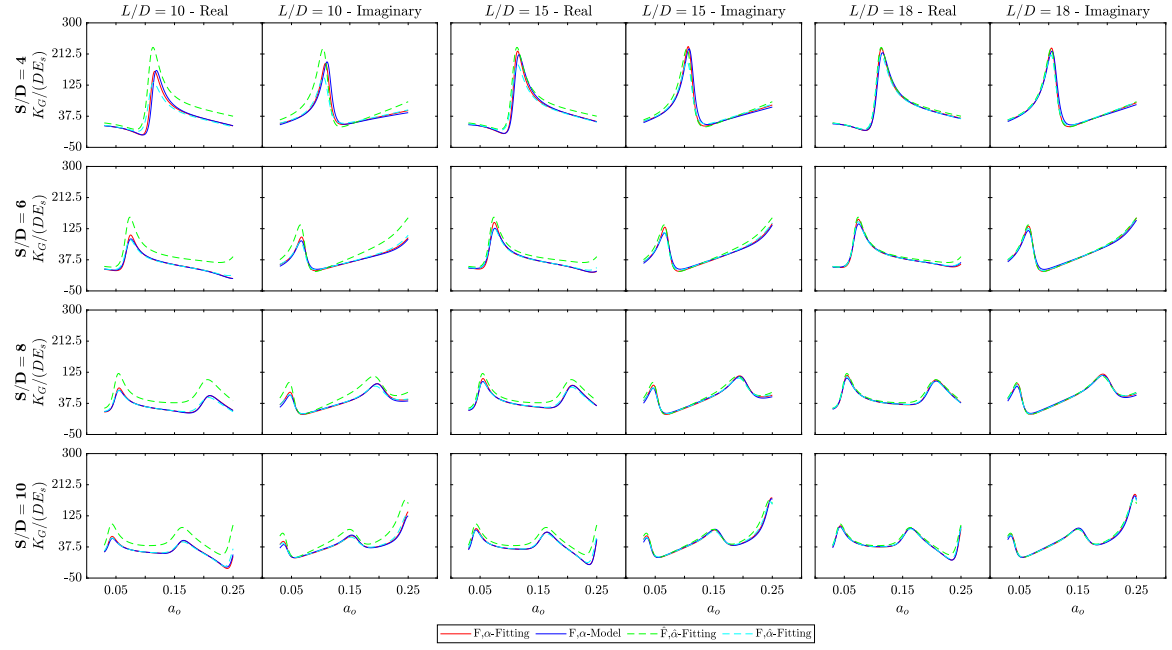

Fig. 9. Vertical 4-pile group impedances for different pile slenderness ratios. (For interpretation of the references to colour in this figure legend, the reader is referred to the web version of this article.)

lowest pile separation and slenderness ratios, $S/D = 4$ and $L/D = 10$). This difference tends to decrease when the pile slenderness and spacing ratios increase. Furthermore, the variations that are produced with the change of the pile slenderness ratio are correctly reproduced with the fits. This fact can be observed when the reference case curve (green dashed lines) is compared with the results corresponding to the pile slenderness variation (continuous lines), especially for the lowest pile slenderness ratio. Note that if the interaction factor expression proposed by Dobry and Gazetas [11] (see Eq. (20)) were used, similar results would be computed for the different pile slenderness ratios, as the expression does not depend on this ratio. Although the pile spacing ratio has not been included as a variable in the fitted expressions of the correction factor, the variation in the results produced by the alteration of the pile spacing ratio is properly reproduced by adjusting the fitted expression of the reference case. Despite the interaction correction factor fits of the pile slenderness ratio have low goodness characteristics (see Table 4), the fitting results match well with the model ones. This is because the flexibility of the source pile (that it is better fitted (see Table 3) has a greater impact on the total dynamic response than the interaction factor). This fact can also be seen when only the flexibility of the source pile is rectified with its correction factors (cyan dashed line), where for separations larger than four times the pile diameter, similar results between this assumption and the superposition of the model flexibilities and interaction factors are obtained. Thus, the contribution of the adjustment of the flexibility of the source pile is quite bigger than the interaction factor one. For the lowest value

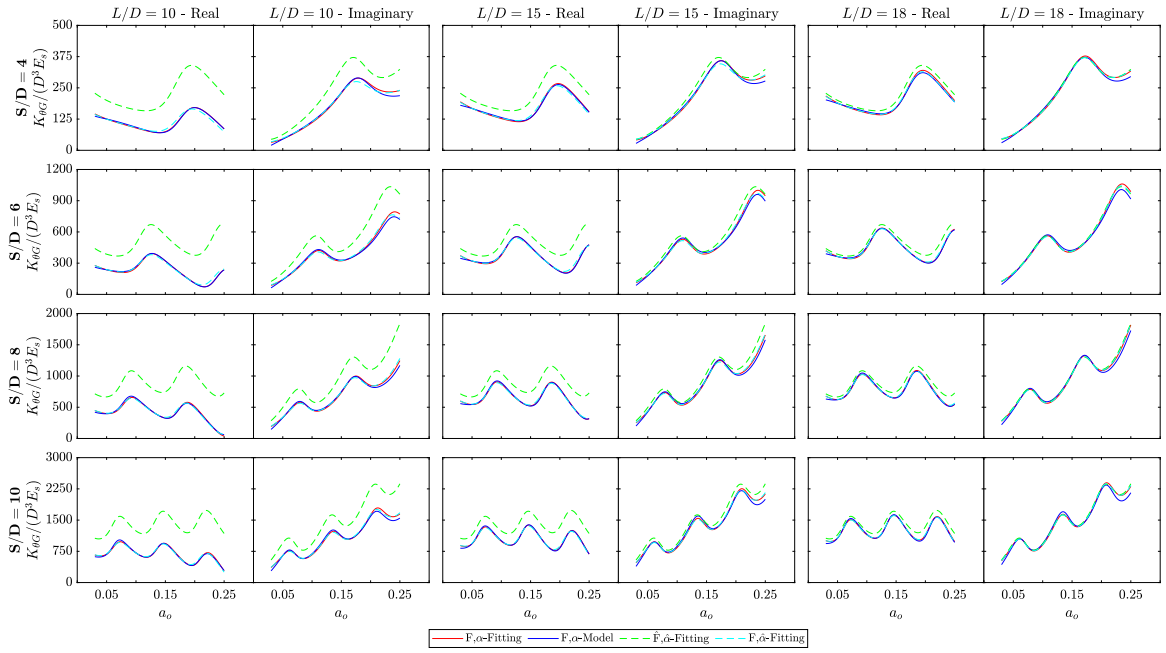

Fig. 10. Rocking 4-pile group impedances for different pile slenderness ratios. (For interpretation of the references to colour in this figure legend, the reader is referred to the web version of this article.)

of the pile spacing ratio it can be observed a phase difference and a considerable difference between this assumption and the model results at the peak impedances, this is due to the greater relevance of pile–pile interaction as the pile spacing ratio decreases.

Fig. 10 shows the dimensionless rocking impedances versus the dimensionless frequency, for different pile slenderness and pile spacing ratios and for the 4-pile group. Results are arranged in the same way as used for the vertical impedances (Fig. 9). The rocking impedances obtained with the superposition of the flexibilities and interaction factors of the proposed expressions match very well with those superimposed with the model flexibilities and interaction factors. In this case, the main differences between the fitting and model results occur at the larger frequencies ($a_o \geq 0.20$) and in the imaginary component, giving slightly greater results the impedances obtained with the fitted expressions. Moreover, the rocking impedances show a greater dependency of the pile slenderness and pile spacing ratios. Note how the differences observed with respect to the reference case are greater than those obtained in the vertical impedances. For these rocking impedances, the assumption of only rectifying the flexibility of the source pile leads to good results, even for the smallest pile spacing ratio. Both in the vertical and rocking impedances, the dynamic vertical group response rises with the increase of the pile slenderness ratio.

– Influence of Young's Modulus ratio

In the same way as previously made for analysing the pile slenderness variation (Figs. 9 and 10), Figs. 11 and 12 show the dimensionless vertical and rocking impedances for different Young's Modulus ($E_p/E_s = 100, 250$ and 500) and pile spacing ratios ($S/D = 4, 6, 8$ and 10), maintaining all other parameters invariant with the values of the reference case ($L/D = 20$ and $\xi_s = 1\%$). The results are presented in the same way that it was exposed for the pile slenderness ratio, showing the impedances for several Young's Modulus ratios in pairs of columns. The vertical impedances obtained through the fitted interaction factors and flexibilities of the source pile align well with the results obtained from the model (see Fig. 11). Only at intermediate Young's Modulus ratios ($E_p/E_s = 100$ and 250) some differences at the first peak and high dimensionless frequencies appear. As it can be observed, the assumption of not considering a correction factor for the argument of the interaction factor in the Young's Modulus ratio practically does not affect the results. As in the previous case (variation of pile slenderness ratio), the alteration due to the Young's Modulus ratio is well captured without adding the pile spacing ratio as a variable in the interaction correction factor fit. Besides, it can be seen that there is a considerable influence of the Young's Modulus ratio in the final results, above all for the lower values of this ratio, in which significant differences can be appreciated comparing the reference case (green dashed line) with the continuous lines. This variation could not be reproduced with the interaction factor expression suggested by Dobry and Gazetas [11] (see Eq. (20)), since this one does not depend on the Young's Modulus ratio. In this case, more differences appear when only the flexibility of the source pile is adjusted with the correction factors (cyan dashed line). These differences can be seen for the lower pile spacing and Young's Modulus ratios, especially, at the first peak, in which a magnitude and phase difference with respect to the continuous lines can be observed. For the rocking impedances (Fig. 12) more differences between the fitting and model curves can be observed, particularly for the higher values of the pile spacing and Young's Modulus ratios, even so the impedances obtained with the fits are quite close to the model ones. When only the adjustment of the flexibility is considered through its correction factors, good results are obtained, although some discrepancies can be seen for the lowest pile spacing and Young's Modulus ratios. What is more, for both the vertical and rocking impedances, larger values of impedances are obtained as the Young's Modulus pile–soil ratio increases.

– Influence of soil damping

The dimensionless vertical and rocking impedances of the 4-pile group for different soil dampings ($\xi_s = 2.5, 5$ and 7.5%) and pile spacing ratios ($S/D = 4, 6, 8$ and 10) are depicted in Figs. 13 and 14 respectively, the other parameters are kept invariant with the values of the reference case ($L/D = 20$ and $E_p/E_s = 500$). Results are shown in the same disposal than the previously used for the pile slenderness and Young's Modulus ratios, but now each pair of columns presents the impedances for each soil damping. Similar conclusions than the previously commented for the pile slenderness and Young's Modulus ratios are also drawn for the soil damping variation: the impedances computed with the fitted interaction factors and flexibilities of the source pile match very well with those of the model in both the vertical

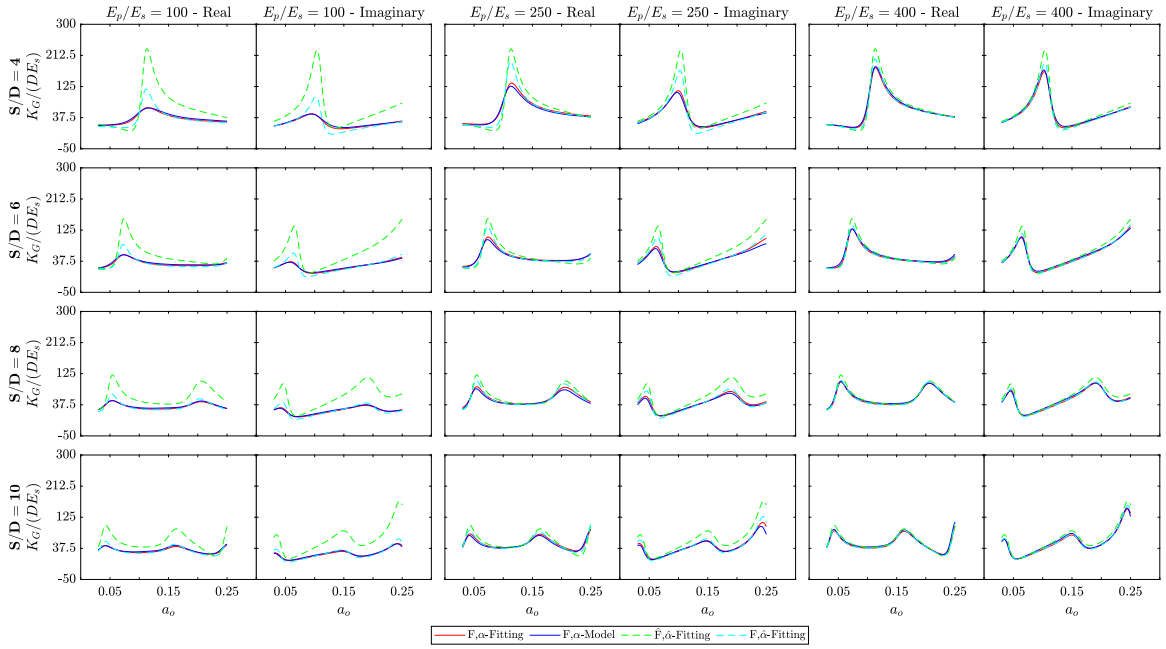

Fig. 11. Vertical 4-pile group impedances for different Young's Modulus ratios. (For interpretation of the references to colour in this figure legend, the reader is referred to the web version of this article.)

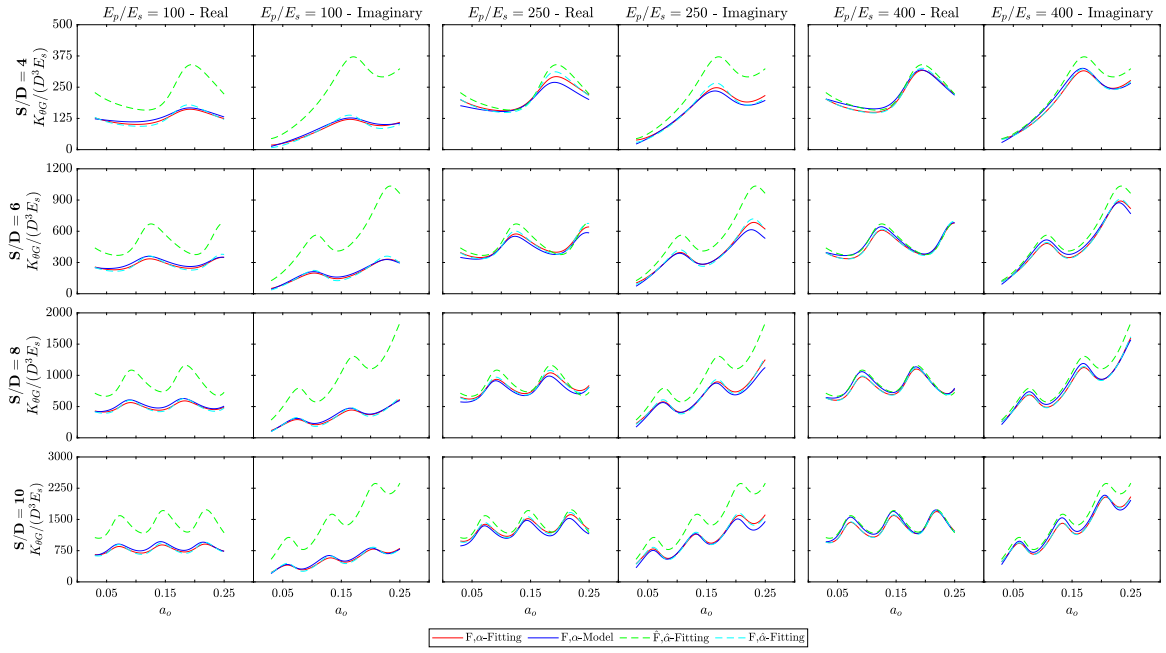

Fig. 12. Rocking 4-pile group impedances for different Young's Modulus ratios. (For interpretation of the references to colour in this figure legend, the reader is referred to the web version of this article.)

and rocking impedances. The larger differences between these two are produced at the first vertical impedance peak and at the highest frequencies in the imaginary component of the rocking impedances. As it can be observed the variation of the soil damping does not significantly affect the vertical and rocking impedances for soil dampings lower than 5%. Nonetheless, for damping values higher than 5%, there are significant differences between the peaks of the reference curve and the peaks of the other curves. The assumption of only considering the correction factors for the flexibility of the source pile allows to obtain good impedances, except for the smallest pile spacing ratio and the soil dampings larger or equal to 5%. For these cases, the contribution of the interaction factor rectification is considerable in order to correctly reproduce the impedance peaks and the frequencies at they occur. Moreover, greater vertical and rocking dynamic impedances are obtained as the soil damping drops off. This fact is due to the attenuation of the pile–pile interaction produced by the increase of the soil damping.

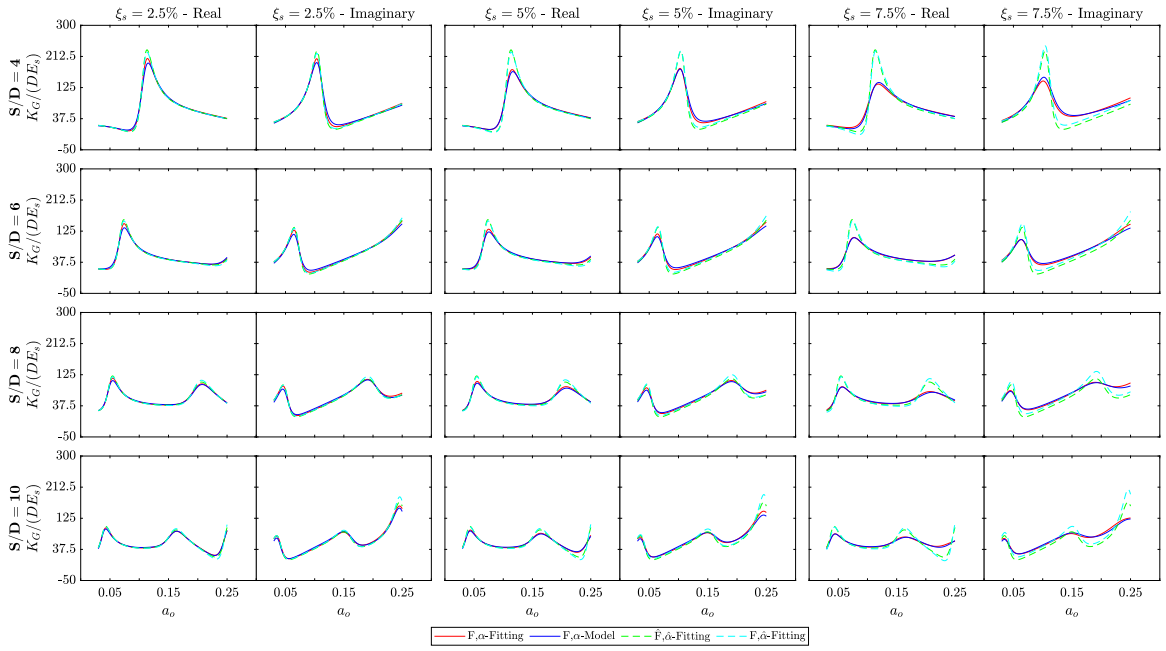

Fig. 13. Vertical 4-pile group impedances for different soil dampings. (For interpretation of the references to colour in this figure legend, the reader is referred to the web version of this article.)

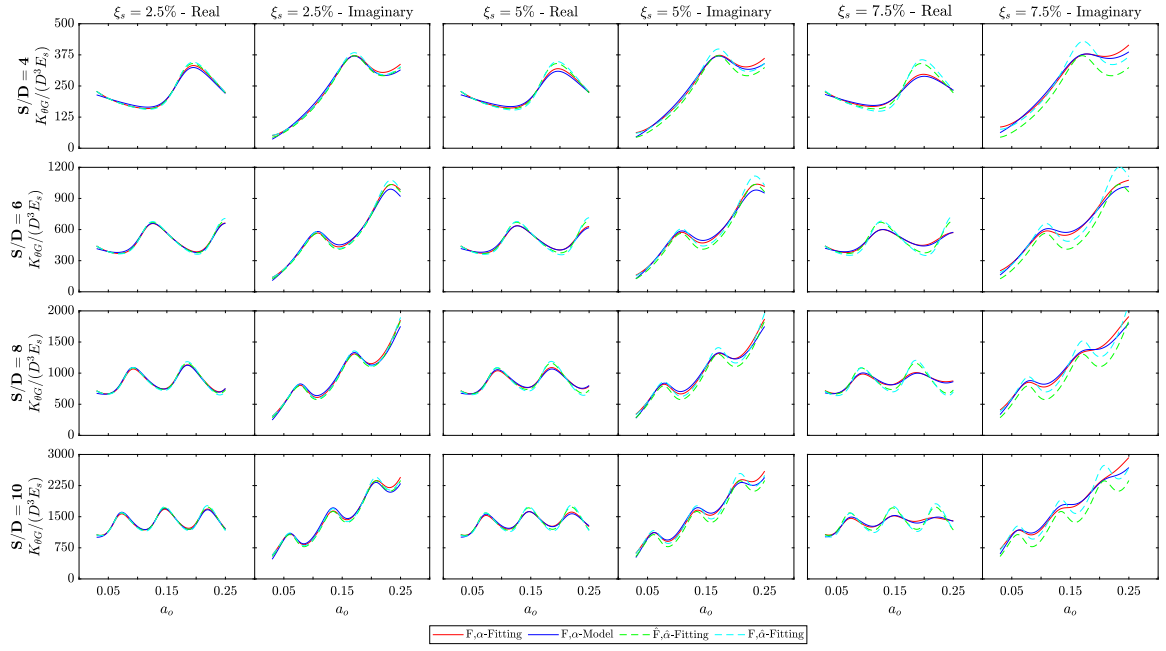

Fig. 14. Rocking 4-pile group impedances for different soil dampings. (For interpretation of the references to colour in this figure legend, the reader is referred to the web version of this article.)

– Variation of the three parameters

Figs. 15 and 16 show the dimensionless vertical and rocking impedances of the 4-pile group against the dimensionless frequency for three different parameter configurations, where the pile slenderness, Young's Modulus ratios and soil dampings are modified at the same time. Specifically, the three studied configurations are: $L/D = 14$, $E_p/E_s = 100$, and $\xi_s = 2\%$; $L/D = 16$, $E_p/E_s = 200$, and $\xi_s = 4\%$; and $L/D = 18$, $E_p/E_s = 400$, and $\xi_s = 5\%$. The results for each configuration are disposed by pair of columns, where the real and imaginary components are represented in the first and second column respectively. The impedances for three different pile spacing ratios ($S/D = 6, 8$ and 10) are arranged by rows. The same curve colours and line traces than those previously used are employed to distinguish the results of the fits and the model. As it is shown, in the first configuration (firsts two columns of Figs. 15 and 16), the fitting and model continuous curves are a little separated from each other, especially for the rocking stiffness (real component) and for the larger pile spacing ratios. Nevertheless, the curve shape is correctly reproduced by using the fitted expressions of the flexibilities of the source pile and interaction factors. Note that this first set of parameters is the furthest from the reference case in terms of pile slenderness and Young's Modulus ratios. However, for the second and third parameter configurations, in which the pile slenderness and Young's Moudulus ratios are nearer to the reference case, the fitting

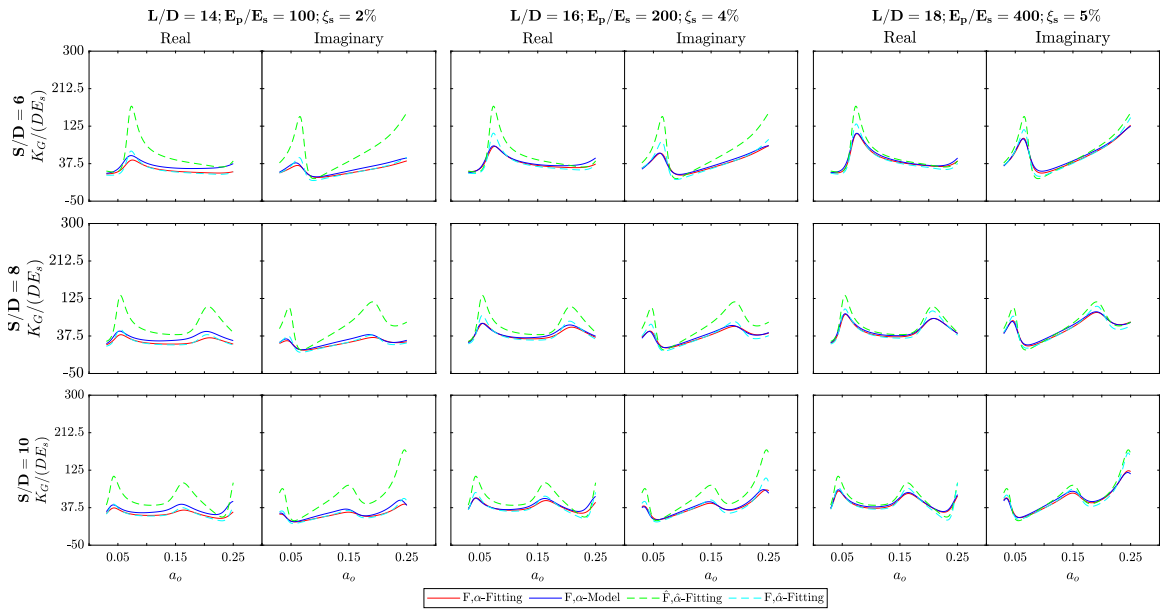

Fig. 15. Vertical 4-pile group impedances for different parameter configurations. (For interpretation of the references to colour in this figure legend, the reader is referred to the web version of this article.)

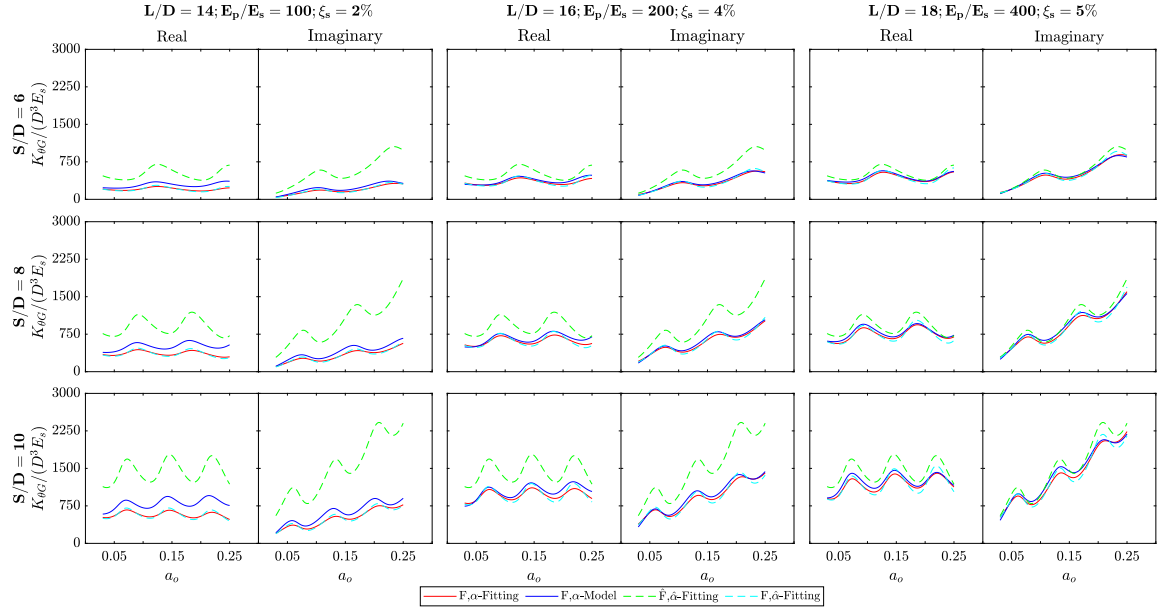

Fig. 16. Rocking 4-pile group impedances for different parameter configurations. (For interpretation of the references to colour in this figure legend, the reader is referred to the web version of this article.)

and model impedances give similar results, both in the vertical and rocking impedances. The impedances computed through the fitted interaction factors and flexibilities of the source pile are commonly lower than those of the model at the entire dimensionless frequency range. For large pile spacing ratios and in the rocking impedances, more differences can be appreciated. Nonetheless, fits generally reproduce well the variation of the group impedances of the reference case. When only the flexibility of the source pile is rectified with the correction factors, it can be seen relevant discrepancies in the peaks of the vertical impedances. These differences are lower in the rocking impedances, but they are noticeable in the two last configurations, which are those that have a greater soil damping.

5. Conclusions

This paper studies the interaction factor superposition method for pile groups of jacket-supported OWTs. The results obtained from this method are compared with those computed by a previously developed continuum model [8]. Ready-to-use expressions are proposed by performing curve fittings for the flexibilities of the source pile and interaction factors directly determined with the continuum model for a wide variety of jacket pile groups parameters. The influence of the dimensionless frequency, pile separation ratio, pile slenderness ratio, Young's Modulus ratios and soil damping is studied and included in the expressions. The validity of these expressions are analysed throughout the work. The following conclusions are drawn:

- The interaction factor superposition method correctly reproduces the vertical and rocking group impedances for the regular pile configurations characteristic of jacket foundations. Thus, for this type of pile groups with large pile spacing ratios, the assumption of only considering the interaction between pile pairs and neglecting the interplay of the other surrounding piles allow to reproduce in a accurately and easily way the dynamic group response. This last consideration is totally fulfilled for pile spacings equal or higher than six times the pile diameter. For lower pile spacings, the rest of piles starts to affect the interaction among the pair of piles, producing differences between the rigorous model and the superposition method.
- Apart from the influence of the dimensionless frequency and separation ratio, the effect of the pile slenderness, Young's Modulus ratios and soil hysteretic damping can be significant in the determination of the impedance functions. The influence of these parameters can be reproduced with the use of correction factors that adapt the flexibilities of the source pile and interaction factors of a reference case. Results obtained with the proposed fitted expressions and correction factors generally reproduce well the dynamic behaviour of pile groups for jacket-supported OWTs. When only one parameter is modified from the reference case, the impedances computed by superimposing the fitted interaction factors and flexibilities of the source pile match quite well with those obtained through the flexibilities and interaction factors of the continuum model. When all parameters are changed at once, greater differences between the results determined with the model and those calculated with the fitted expressions are obtained. Especially when the pile slenderness and Young's Modulus ratios are far from the reference case values ($L/D = 20$ and $E_p/E_s = 500$). However, these differences are acceptable and the curve shape is properly reproduced.
- The assumption of only adjusting the flexibility of the source pile with the proposed correction factors can lead to admissible vertical and rocking impedances. The rocking impedances obtained with this simplification are generally acceptable. Nevertheless, for low values of pile spacing and Young's Modulus ratios, as well as for large values of soil dampings, omitting the influence of these parameters on the interaction factors can lead to significant differences in the vertical impedances, especially in their peak values.

Thus, the dynamic vertical response of jacket pile groups can be estimated applying the interaction factor superposition method and the proposed expressions. The use of this method and the proposed expressions are useful since they can be employed without the need to execute a rigorous model, allowing to obtain the vertical and rocking impedances in a faster and simpler way. These impedances could subsequently be used to reproduce the soil–structure interaction of these type of structures. As future developments it is proposed to carry out a similar work but analysing the horizontal and rocking-horizontal dynamic behaviour of jacket pile groups. Additionally, this study can be extended to more complex soils, such as stratified or saturated soils. Furthermore, it could be interesting to evaluate the superposition method by employing more complex techniques, such as machine learning, that could improve the proposed expressions. For instance, artificial neural networks combined with the proposed superposition procedure could result in more accurate impedance functions. Artificial networks could be used to predict the own vertical flexibilities and interaction factors, considering all relevant soil and pile variables at once. Then, the impedance functions would be computed applying elastic superposition.

CRediT authorship contribution statement

Eduardo Rodríguez-Galván: Writing – original draft, Visualization, Software, Methodology, Conceptualization. **Guillermo M. Álamo:** Writing – review & editing, Supervision, Software, Conceptualization. **Juan J. Aznárez:** Writing – review & editing, Supervision, Funding acquisition, Conceptualization. **Orlando Maeso:** Writing – review & editing, Supervision, Conceptualization.

Declaration of competing interest

The authors declare that they have no known competing financial interests or personal relationships that could have appeared to influence the work reported in this paper.

Acknowledgements

This research has been funded by Ministerio de Ciencia e Innovación and Agencia Estatal de Investigación (MCIN/AEI/10.13039/501100011033) of Spain through research project PID2020-120102RBI00 and predoctoral research scholarship PRE2021-099200 (E. Rodríguez-Galván), also funded by FSE+. This research has been partially supported by ACIISI, Spain-Gobierno de Canarias and European FEDER Funds Grant EIS 2021 04.

Data availability

Data will be made available on request.

References

[1] Council GWE. Global offshore wind report 2023. Brussels, Belgium: GWEC 2023.
[2] Musial W, Spitsen P, Duffy P, Beiter P, Shields M, Mulas Hernando D, Hammond R, Marquis M, King J, Sathish S. Offshore wind market report: 2023 edition. Tech. rep., National Renewable Energy Laboratory (NREL), Golden, CO (United States); 2023.
[3] Jalbi S, Bhattacharya S. Concept design of jacket foundations for offshore wind turbines in 10 steps. Soil Dyn Earthq Eng 2020;139:106357.
[4] Kaynia AM. Dynamic stiffness and seismic response of pile groups (Ph.D. thesis), Massachusetts Institute of technology; 1982.
[5] Kaynia AM, Kausel E. Dynamics of piles and pile groups in layered soil media. Soil Dyn Earthq Eng 1991;10(8):386–401.
[6] Dezi F, Carbonari S, Leoni G. A model for the 3D kinematic interaction analysis of pile groups in layered soils. Earthq Eng Struct Dyn 2009;38(11):1281–305.
[7] Dezi F, Carbonari S, Morici M. A numerical model for the dynamic analysis of inclined pile groups. Earthq Eng Struct Dyn 2016;45(1):45–68.
[8] Álamo GM, Martínez-Castro AE, Padrón LA, Aznárez JJ, Gallego R, Maeso O. Efficient numerical model for the computation of impedance functions of inclined pile groups in layered soils. Eng Struct 2016;126:379–90.
[9] Wang P, Huang Y, Zhao M, Cheng X, Du X. Analytical solution for simplifying the pile-soil interaction to a spring-damping system under horizontal vibration. Soils Found 2024;64(3):101469.
[10] Poulos HG. Analysis of the settlement of pile groups. Geotech 1968;18(4):449–71.
[11] Dobry R, Gazetas G. Simple method for dynamic stiffness and damping of floating pile groups. Geotech 1988;38(4):557–74.
[12] Gazetas G, Makris N. Dynamic pile-soil-pile interaction. Part I: Analysis of axial vibration. Earthq Eng Struct Dyn 1991;20(2):115–32.
[13] Mylonakis G, Gazetas G. Settlement and additional internal forces of grouped piles in layered soil. Geotech 1998;48(1):55–72.
[14] Makris N, Gazetas G. Dynamic pile-soil-pile interaction. Part II: Lateral and seismic response. Earthq Eng Struct Dyn 1992;21(2):145–62.
[15] Rotta Loria AF, Laloui L. The interaction factor method for energy pile groups. Comput Geotech 2016;80:121–37.
[16] Gazetas G, Fan K, Kaynia AM. Dynamic response of pile groups with different configurations. Soil Dyn Earthq Eng 1993;12(4):239–57.
[17] Torshizi MF, Saitoh M, Álamo GM, Goit CS, Padrón LA. Influence of pile radius on the pile head kinematic bending strains of end-bearing pile groups. Soil Dyn Earthq Eng 2018;105:184–203.
[18] Zheng C, Cui Y, Kouretzis G, Luan L. Scattered wave effects on the vertical dynamic response of pile groups embedded in layered soil. Comput Geotech 2023;158:105361.
[19] Sales MM, Curado TS. Interaction factor between piles: limits on using the conventional elastic approach in pile group analysis. Soil. Rocks 2018;41(1):49–60.
[20] Mylonakis G. Contributions to static and seismic analysis of piles and pile-supported bridge piers. State University of New York at Buffalo; 1995.

[21] Abhinav KA, Saha N. Coupled hydrodynamic and geotechnical analysis of jacket offshore wind turbine. Soil Dyn Earthq Eng 2015;73:66–79.
[22] Jalbi S, Bhattacharya S. Closed form solution for the first natural frequency of offshore wind turbine jackets supported on multiple foundations incorporating soil-structure interaction. Soil Dyn Earthq Eng 2018;113:593–613.
[23] Plodpradit P, Dinh VN, Kim K-D. Coupled analysis of offshore wind turbine jacket structures with pile-soil-structure interaction using FAST v8 and X-SEA. Appl Sci 2019;9(8):1633.
[24] Romero-Sánchez C, Padrón LA. Influence of wind and seismic ground motion directionality on the dynamic response of four-legged jacket-supported Offshore Wind Turbines. Eng Struct 2024;300:117191.
[25] Quevedo-Reina R, Álamo GM, François S, Lombaert G, Aznárez JJ. Importance of the soil–structure interaction in the optimisation of the jacket designs of offshore wind turbines. Ocean Eng 2024;303:117802.
[26] Álamo GM, Bordón JDR, Aznárez JJ. On the application of the beam model for linear dynamic analysis of pile and suction caisson foundations for offshore wind turbines. Comput Geotech 2021;134:104107.
[27] API RP 2A-WSD. Recommended practice for planning, designing and constructing fixed, offshore plaftorms - working stress design. American Petroleum Institute.